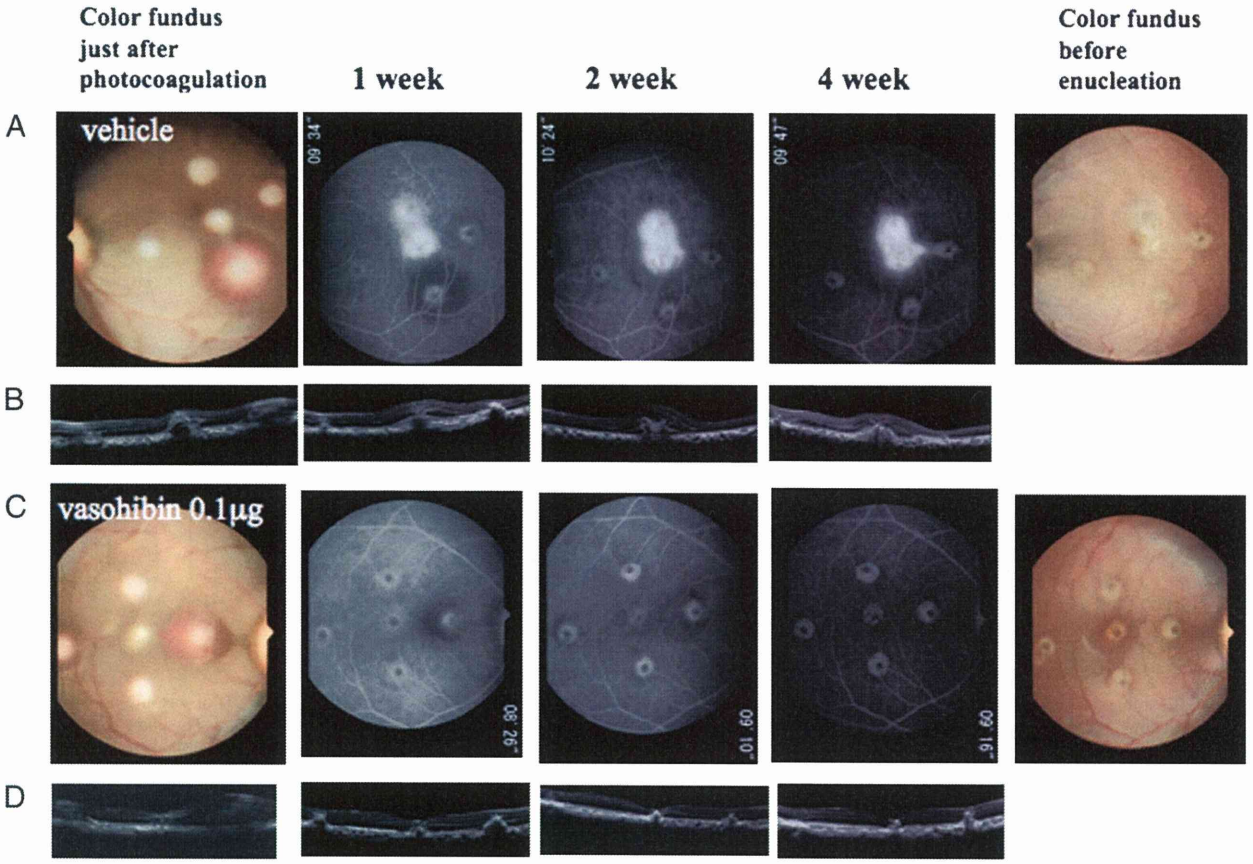

COLOR

Fig. 3. Fluorescein angiograms, ocular coherence tomographic images, color fundus photographs, and focal ERGs are shown. Vasohibin-1 (0.1 μg/50 μL) was injected into the vitreous of the right eyes 3 times on 0, 4, and 7 days after laser application, and the same amount of vehicle was injected into left eyes on the same days. Photographs show the fundus just after the laser application and the day of enucleation. Fluorescein angiographs recorded 1, 2, and 4 weeks after laser application. Photographs of the right (**A**) and left (**C**) eyes are shown. The results of OCT on the indicated days are shown in the same vertical columns for the indicated day (**B**) and (**D**).

numbers of macrophage-like cells were also observed in the neural retina.[21]

In immunostained eyes, vasohibin-1 positivity was found mainly in the CNV especially on the ECs in the CNV (Figure 5B). The regions surrounding the CNV showed little vasohibin-1–positive staining. Some monkeys showed no vasohibin-1 expression by immunohistochemistry even in the CNV at 28 day after laser application. Positive staining for vasohibin-1 appeared to be greater in the more active CNVs (Figure 5A), and it was more obvious in nontreated monkey eyes, although we could not determine whether the staining was significantly greater because only 3 monkey eyes were studied.

Vascular Endothelial Growth Factor in Aqueous During Experiments

The level of VEGF was determined by enzyme-linked immunosorbent assay. The average VEGF level in the aqueous in the vasohibin-1–injected eyes was 15.3 pg/mL, and it was 20.6 pg/mL in the vehicle-treated eyes at 4 days after laser application. The average VEGF level in the vasohibin-1– and vehicle-treated eyes were 7.0 pg/mL and 8.9 pg/mL, respectively, at 4 weeks after laser application (Figure 6). For both times, the differences were not significant.

Discussion

Our results demonstrated that when 10 μg or 100 μg of vasohibin-1 was injected intravitreally into nontreated normal monkey eyes, a mild anterior chamber inflammation developed. No signs of inflammation or any adverse effects were found when <1 μg of vasohibin-1 was injected into nonlaser treated eyes, although we used only 1 eye for each dose. However when 1 μg of vasohibin-1 was injected into laser-treated eyes, a mild inflammation developed in 1 of the 3 eyes. Inflammation has also been reported in monkey

COLOR

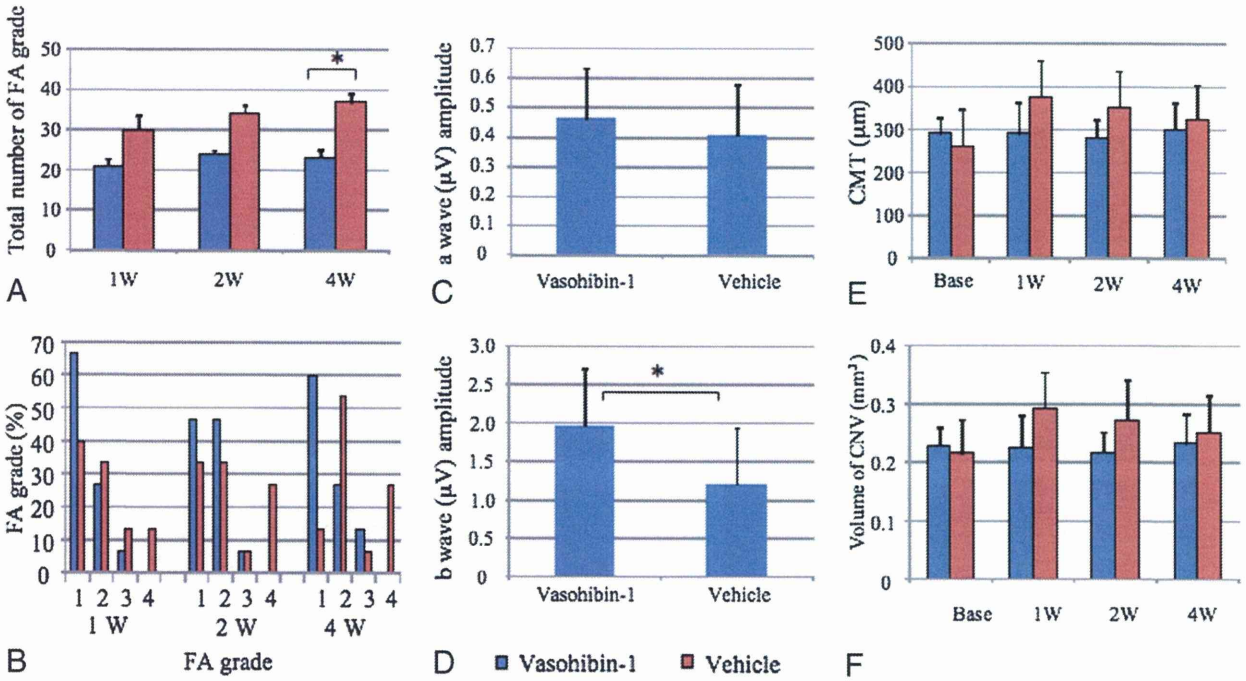

Fig. 4. Results of FA, focal ERG, and OCT are shown. **A.** Significantly less FA leakage was observed after 0.1 μg/50 μL of vasohibin-1 than after vehicle treatment at 4 weeks. **B.** Distribution of Grade 4 FA eyes for each group. **C** and **D.** Average amplitudes of the a-waves (**C**) and b-waves (**D**) of the focal ERGs. **E** and **F.** Average central macular thickness (CMT) and the central 3.4 mm and volume of area of either vasohibin-1–treated (blue) or vehicle-treated (red) eyes before (base) and 1, 2, and 4 weeks after laser application. Lower thickness and volumes were observed in the vasohibin-1–treated monkeys. Data are the standard deviations.

eyes after intravitreal injections of fragments of mouse and human chimera antibodies against VEGF.[22,27]

Fluorescein angiography examination after vasohibin-1 injection in laser-treated eyes showed significantly lower FA scores in eyes that received 0.1 μg and 1 μg of vasohibin-1 than the vehicle-injected eyes, although the number of eyes may have affected the statistics. Fluorescein leakage from the laser spots close to the macula was greater than that of the other laser spots. These results are compatible with the results of Shen et al,[28] who also found that the laser spot was larger and the leakage was greater for lesions closer to the macula. We also found that fluorescein leakage was different among monkeys, even though we applied the same amount of vasohibin-1.[22] This variability may be because the body weight ranged from 4.1 kg to 10.1 kg and age from 4 years to 6 years among the monkeys.

After we injected 0.1 μg of vasohibin-1 3 times in the right eyes and vehicle into the left eyes of 3 monkeys, we found significantly less fluorescein leakage in the vasohibin-1–treated right eyes than in the vehicle-treated eyes. The results of focal ERGs and OCT were well correlated with the results of FA findings, although the quantitative values were not significantly different.

Taken together, these results showed that intravitreal vasohibin-1 is able to reduce the activity of the laser-induced CNV in monkeys. With 3 injections of 0.1 μg of vasohibin-1, the results were not so different from that of only 1 injection at 4 days after the laser application. This may indicate that there may be an optimum time for the vasohibin-1 to affect the course of the laser-induced CNV. Alternatively, the results may be related to the half-life of vasohibin-1.

We found that vasohibin-1 was expressed on ECs especially those in the CNV lesions. Careful examinations showed that vasohibin-1 expression was limited to the CNV lesion and may not show extensive expression in other regions under normal physiologic conditions. Although we have not followed the expression of vasohibin-1 during the course of CNV development in monkeys, vasohibin-1 expression may be enhanced in the new vessels as was reported.[29] The vasohibin-1 expression appeared stronger in non-treated monkey eyes, although this could not be quantified. Vasohibin-1 has been reported to be present on the ECs only in the stroma of tumors and not in the noncancerous regions of the tissue in surgically resected tissues of the same patient.[29] These findings suggest that vasohibin-1 may be expressed mainly in the new vessels as it was in our laser-induced CNVs.

COLOR

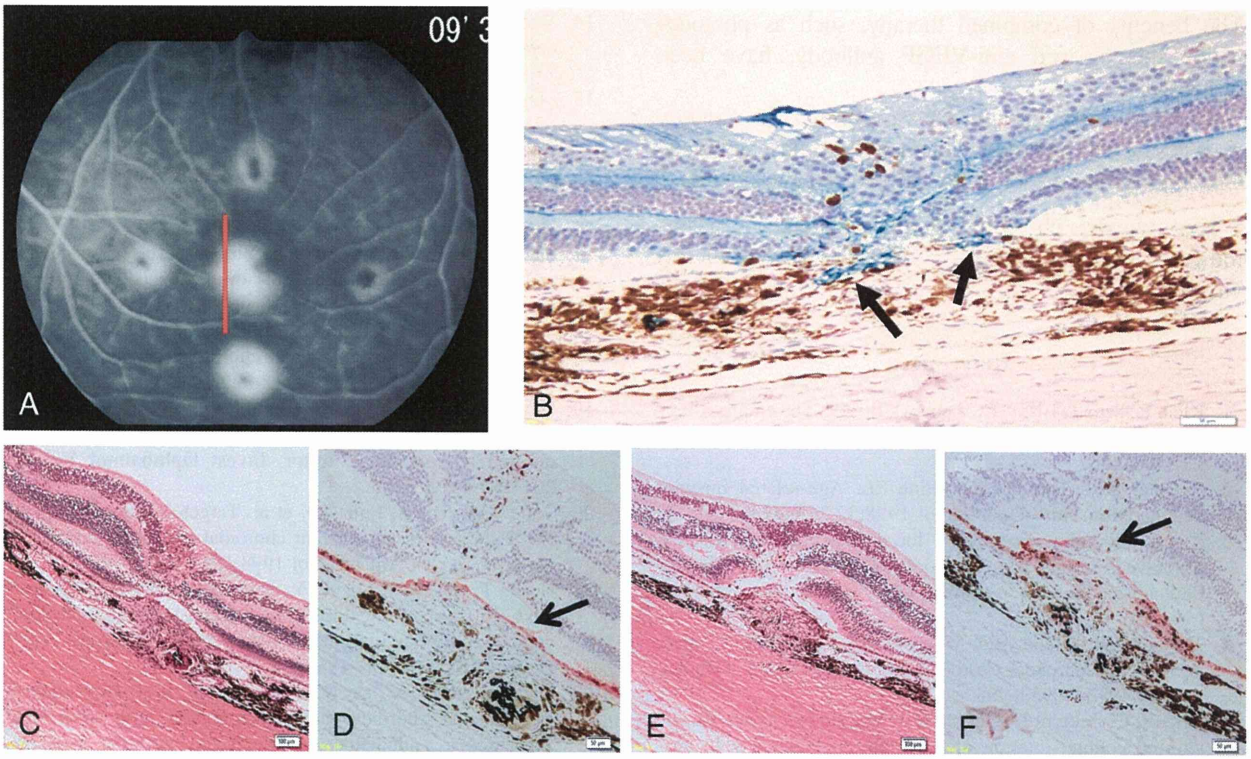

Fig. 5. Fluorescein angiograms 4 weeks after laser application or vehicle injection are shown. **A.** Immunohistochemistry for vasohibin-1 (**B**), the same eye as shown in (**A**) at the red line, is shown. Arrows indicate vasohibin-1 labeling. Vasohibin-1 expression is concentrated on the vessels around the CNV (arrows), but markedly less than in the CNV. Vaoshibin-1 expression was observed at active CNV (red line in **A**). The subretinal space is an artifact of histologic processing. Cytokeratin labeling is also shown with vasohibin-treated eye (**D**) and vehicle-treated eye (**F**). Arrows show labeling of cytokeratin. Bar = 50 μm. **C** and **E.** Hematoxylin and eosin staining of vasohibin-1–treated and vehicle-treated eyes, respectively, are shown. Bar = 100 μm. Cytokeratin labeling shows that retinal pigment epithelium covers CNV in the vasohibin-1–treated eyes (**D**), and a disruption of cytokeratin labeling is observed in vehicle-treated eye (**F**).

Hosaka et al[29] reported that exogenous vasohibin-1 blocked angiogenesis and maturation of not only the cancerous tissue but also the surrounding vessels and, thus, enhanced the antitumor effects of vasohibin-1. Intravitreal injection of vasohibin-1 may also suppress angiogenesis in CNVs by the same mechanism.

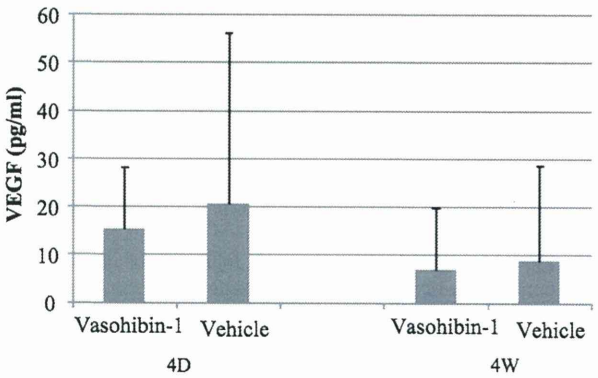

Fig. 6. Concentration of VEGF in aqueous in laser-treated monkey eyes 4 days and 4 weeks after laser application is shown. Vertical axis shows VEGF concentration in picograms per milliliter, and horizontal axis is the day of examination. Vascular endothelial growth factor in vasohibin-1–treated eyes (blue boxes) and vehicle-treated eyes (red boxes) show no significant difference at any times.

The amount of VEGF in the aqueous in the vasohibin-1–treated eyes did not differ from that in vehicle-treated eyes. Thus, Zhou et al[30] reported that external vasohibin-1 had no effect on the level of VEGF when they used adenovirus encoding human vasohibin-1 on mouse corneal neovascularization induced by alkali burn. They also reported that vasohibin-1 may downregulate the VEGF receptor 2 (VEGFR2). Shen et al[16] also reported a downregulation of VEGFR2 by vasohibin-1 during mouse ischemic retinopathy. Our previous studies have also shown a downregulation of VEGFR2 by external vasohibin-1 in laser-induced mouse CNVs.[19] Thus, vasohibin-1 may reduce the activity of a CNV by partially downregulating VEGFR2 in the eyes. If this is correct, vasohibin-1 may not affect the favorable aspects of VEGF such as its neuroprotective effect,[31] especially if VEGF works through VEGFR1 rather than VEGFR2. Vasohibin-1 also can be used with anti-VEGF antibody for CNV therapy.

The benefits of combined therapy, such as photodynamic therapy and anti-VEGF antibody, have been discussed.[27]

In conclusion, intravitreal vasohibin-1 in monkey eyes is safe and can reduce the activity of laser-induced CNVs and thus preserve the function of the macula.

Key words: choroidal neovascularization, laser-induced, monkey, vascular endothelial growth factor, vasohibin-1.

References

1. Klein R, Peto T, Bird AC, Vannewkirk MR. The epidemiology of age-related macular degeneration. Am J Ophthalmol 2004; 137:486–495.
2. Bressler NM, Bressler SB, Fine SL. Age-related macular degeneration. Surv Ophthalmol 1998;32:375–413.
3. Argon laser photocoagulation for neovascular maculopathy. Three-year results from randomized clinical trials Macular Photocoagulation Study Group. Arch Ophthalmol 1986;104: 694–701.
4. Thomas MA, Grand MG, Williams DF, et al. Surgical management of subfoveal choroidal neovascularization. Ophthalmology 1992;99:952–968.
5. Eckardt C, Eckardt U, Conrad HG. Macular rotation with and without counter-rotation of the globe in patients with age-related macular degeneration. Graefes Arch Clin Exp Ophthalmol 1999;237:313–325.
6. Reichel E, Berrocal AM, Ip M, et al. Transpupillary thermotherapy of occult subfoveal choroidal neovascularization in patients with age-related macular degeneration. Ophthalmology 1999; 106:1908–1914.
7. Photodynamic therapy of subfoveal choroidal neovascularization in age-related macular degeneration with verteporfin: one year results of 2 randomized clinical trials-TAP report Treatment of Age-related Macular Degeneration with Photodynamic Therapy (TAP). Study Group. Arch Ophthalmol 1999;117:1329–1345.
8. Grisanti S, Tatar O. The role of vascular endothelial growth factor and other endogenous interplayers in age-related macular degeneration. Prog Retin Eye Res 2008;27:372–390.
9. Miller JW, Adamis AP, Shima DT, et al. Vascular endothelial growth factor/vascular permeability factor is temporally and spatially correlated with ocular angiogenesis in a primate model. Am J Pathol 1994;145:574–584.
10. Krzystolik MG, Afshari MA, Adamis AP, et al. Prevention of experimental choroidal neovascularization with intravitreal anti-vascular endothelial growth factor antibody fragment. Arch Ophthalmol 2002;120:338–346.
11. Rosenfeld PJ, Brown DM, Heier JS, et al. Ranibizumab for neovascular age-related macular degeneration. N Engl J Med 2006;355:1419–1431.
12. Pilli S, Kotsolis A, Spaide RF, et al. Endophthalmitis associated with intravitreal anti-vascular endothelial growth factor therapy injections in an office setting. Am J Ophthalmol 2008;145:879–882.
13. Lux A, Llacer H, Heussen FMA, Joussen AM. Non-responders to bevacizumab (Avastin) therapy of choroidal neovascular lesions. Am J Ophthalmol 2007;91:1318–1322.
14. Watanabe K, Hasegawa Y, Yamashita H, et al. Vasohibin as an endothelium-derived negative feedback regulator of angiogenesis. J Clin Invest 2004;114:898–907.
15. Shimizu K, Watanabe K, Yamashita H, et al. Gene regulation of a novel angiogenesis inhibitor, vasohibin, in endothelial cells. Biochem Biophys Res Commun 2005;327:700–706.
16. Shen J, Yang X, Xiao WH, et al. Vasohibin is up-regulated by VEGF in the retina and suppresses VEGF receptor 2 and retinal neovascularization. FASEB J 2006;20:723–725.
17. Sato H, Abe T, Wakusawa R, et al. Vitreous levels of vasohibin-1 and vascular endothelial growth factor in patients with proliferative diabetic retinopathy. Diabetologia 2009;52:359–361.
18. Wakusawa R, Abe T, Sato H, et al. Expression of vasohibin, an antiangiogenic factor, in human choroidal neovascular membranes. Am J Ophthalmol 2008;146:235–243.
19. Wakusawa R, Abe T, Sato H, et al. Suppression of choroidal neovascularization by vasohibin-1, vascular endothelium-derived angiogenic inhibitor. Invest Ophthalmol Vis Sci 2011;52:3272–3280.
20. Tobe T, Ortega S, Luna JD, et al. Targeted disruption of the FGF2 gene does not prevent choroidal neovascularization in a murine model. Am J Pathol 1998;153:1641–1646.
21. Heishi T, Hosaka T, Suzuki Y, et al. Endogenous angiogenesis inhibitor vasohibin1 exhibits broad-spectrum antilymphangiogenic activity and suppresses lymph node metastasis. Am J Pathol 2010;176:1950–1958.
22. Krzystolik MG, Afshari MA, Adamis AP, et al. Prevention of experimental choroidal neovascularization with intravitreal anti-vascular endothelial growth factor antibody fragment. Arch Ophthalmol 2002;120:338–346.
23. Miyake Y, Yanagida K, Yagasaki K, et al. Subjective scotometry and recording of local electroretinogram and visual evoked response. System with television monitor of the fundus. Jpn J Ophthalmol 1981;25:439–448.
24. Kondo M, Ueno S, Piao CH, et al. Comparison of focal macular cone ERGs in complete-type congenital stationary night blindness and APB-treated monkeys. Vision Res 2008;48: 273–280.
25. Hogan MJ, Kimura SJ, Thygeson P. Signs and symptoms of uveitis. I. Anterior uveitis. Am J Ophthalmol 1959;47:155–170.
26. Zhang M, Zhang J, Yan M, et al. Recombinant anti-vascular endothelial growth factor fusion protein efficiently suppresses choroidal neovascularization in monkeys. Mol Vision 2008;14:37–49.
27. Husain D, Kim I, Gauthier D, et al. Safety and efficacy of intravitreal injection of ranibizumab in combination with verteporfin PDT on experimental choroidal neovascularization in the monkey. Arch Ophthalmol 2005;123:509–516.
28. Shen WY, Lee SY, Yeo I, et al. Predilection of the macular region to high incidence of choroidal neovascularization after intense laser photocoagulation in the monkey. Arch Ophthalmol 2004;122:353–360.
29. Hosaka T, Kimura H, Heishi T, et al. Vasohibin-1 expression in endothelium of tumor blood vessels regulates angiogenesis. Am J Pathol 2009;175:430–439.
30. Zhou SY, Xie ZL, Xiao O, et al. Inhibition of mouse alkali burn induced-corneal neovascularization by recombinant adenovirus human vasohibin-1. Mol Vision 2010;16:1389–1398.
31. Alon T, Hemo I, Itin A, et al. Vascular endothelial growth factor acts as a survival factor for newly formed retinal vessels and has implications for retinopathy of prematurity. Nat Med 1995;1:1024–1028.

Suppression of Choroidal Neovascularization by Vasohibin-1, a Vascular Endothelium–Derived Angiogenic Inhibitor

Ryosuke Wakusawa,[1,2] *Toshiaki Abe,*[1] *Hajime Sato,*[2] *Hikaru Sonoda,*[3] *Masaaki Sato,*[3] *Yuuichi Mitsuda,*[3] *Tomoaki Takakura,*[3] *Tomi Fukushima,*[3] *Hideyuki Onami,*[1,2] *Nobuhiro Nagai,*[1] *Yumi Ishikawa,*[1] *Kohji Nishida,*[2] *and Yasufumi Sato*[4]

Purpose. To determine the expression of vasohibin-1 during the development of experimentally induced choroidal neovascularization (CNV) and to investigate the effect of vasohibin-1 on the generation of CNV.

Methods. CNV lesions were induced in the eyes of wild-type (WT) and vasohibin-1 knockout (KO) mice by laser photocoagulation. The expression of vasohibin-1, vascular endothelial growth factor (VEGF), VEGF receptor-1 (VEGFR1), VEGFR2, and pigment epithelial–derived factor (PEDF) was determined by semiquantitative reverse transcription-polymerase chain reaction. The expression of vasohibin-1 was also examined by immunohistochemistry with anti-CD68, anti-alpha smooth muscle actin (αSMA), anti-cytokeratin, and anti-CD31. Vasohibin-1 was injected into the vitreous and the activity and size of the CNV were determined by fluorescein angiography and in choroidal flat mounts.

Results. Vasohibin-1 was detected not only in CD31-positive endothelial cells but also in CD68-positive macrophages and αSMA-positive retinal pigment epithelial cells. Strong vasohibin-1 expression was observed at day 28, when the CNV lesions had regressed by histologic examination. The vasohibin-1 level was significantly decreased at day 14 and increased at day 28 after laser application. Significantly less VEGFR2 expression was observed on day 4 after vasohibin-1. The expression of PEDF was not significantly changed by vasohibin-1 injection. Vasohibin-1 injection significantly suppressed the CNV, with no adverse side effects. The CNV lesions in the vasohibin-1-KO mice were significantly larger than those in the WT mice.

Conclusions. The endogenous expression of vasohibin-1 is associated with the natural course of the development of CNV. Intravitreal injections of vasohibin-1 may be a method for inhibiting CNV. (*Invest Ophthalmol Vis Sci.* 2011;52:3272–3280) DOI:10.1167/iovs.10-6295

The most common cause of central vision loss in the elderly population of developed countries is age-related macular degeneration (AMD), and the cause of the vision loss in the exudative form of AMD is choroidal neovascularization (CNV).[1] CNV leads to subretinal hemorrhages, exudative lesions, serous retinal detachment, and disciform scars.[2]

Vascular endothelial cells (ECs), retinal pigment epithelial (RPE) cells, and macrophage-like mononuclear cells are the major cellular components of CNV membranes, and they produce many types of proangiogenic and antiangiogenic factors.[3–10] Vascular endothelial growth factor (VEGF), a proangiogenic factor, plays a major role in the development of CNV.[11]

Experimental studies have led to the development of anti-VEGF treatments for patients with AMD,[10,12,13] and such therapies are being successfully used. However, there are some disadvantages of VEGF therapy. First, monthly administration of anti-VEGF is necessary to maintain stable vision.[14] The repeated intravitreal injections are stressful for patients and doctors and can lead to irritation, infection, and other side effects.[15] Second, not all patients respond to VEGF therapy.[16] Third, anti-VEGF therapy blocks the antiapoptotic activity of VEGF, which is essential for the survival of the vascular ECs and nonvascular cells developmentally and in adults.[17,18] Indeed, VEGF is essential for the maintenance of the choriocapillaris and neural retina.[19–21] However, it is still being debated whether a prolonged blockade of VEGF will alter the systemic and ocular homeostasis.[15,22,23] Because of the adverse effects of anti-VEGF therapy, anti-VEGF antibody should be used with caution and other antiangiogenic agents should be considered.

Vasohibin-1 is a VEGF-inducible gene in human cultured ECs and has antiangiogenic properties.[24,25] The antiangiogenic properties were noted after it was shown that recombinant vasohibin-1 inhibited the network formation of ECs in vitro and also inhibited retinal neovascularization in a mouse model of oxygen-induced ischemic retinopathy.[24,26] Vasohibin-1 differs from other angiogenesis inhibitors by being selectively induced in ECs by proangiogenic factors such as VEGF and basic fibroblast growth factor (bFGF).[24,27] Thus, vasohibin-1 is considered to be an intrinsic and highly specific negative feedback regulator of activated ECs engaged in angiogenesis.

We recently found that vasohibin-1 is expressed in the CNV membranes obtained from human eyes with AMD.[28] Of note, eyes with lower ratios of vasohibin-1 to VEGF expression tended to have larger subretinal hemorrhages and vitreous hemorrhages,

From the [1]Division of Clinical Cell Therapy, Center for Advanced Medical Research and Development, the [2]Department of Ophthalmology and Visual Science, and the [3]Department of Vascular Biology, Institute of Development, Aging, and Cancer, Tohoku University Graduate School of Medicine, Miyagi, Japan; and the [4]Discovery Research Laboratories, Shionogi and Co. Ltd, Osaka, Japan.

Supported in part by Grants-in-Aid for Scientific Research 21592214 and 20592030 (TA) from the Japan Society for the Promotion of Science, Chiyoda-ku, Tokyo, Japan

Submitted for publication July 28, 2010; revised November 30, 2010, and January 28, 2011; accepted January 30, 2011.

Disclosure: **R. Wakusawa**, None; **T. Abe**, None; **H. Sato**, None; **H. Sonoda**, None; **M. Sato**, None; **Y. Mitsuda**, None; **T. Takakura**, None; **T. Fukushima**, None; **H. Onami**, None; **N. Nagai**, None; **Y. Ishikawa**, None; **K. Nishida**, None; **Y. Sato**, None

Corresponding author: Toshiaki Abe, Division of Clinical Cell Therapy, United Center for Advanced Research and Translational Medicine (ART), Tohoku University, Graduate School of Medicine, 1-1 Seiryoumachi Aobaku Sendai, Miyagi, 980-8574 Japan; toshi@oph.med.tohoku.ac.jp.

Investigative Ophthalmology & Visual Science, May 2011, Vol. 52, No. 6

whereas eyes with a higher vasohibin-1/VEGF ratio had subretinal fibrosis-like lesions.

The purpose of this study was to examine the vasohibin-1 expression during the development of experimentally induced CNV and to investigate the effect of vasohibin-1 on the generation of a CNV. To accomplish this, we first examined the expression of vasohibin-1 during the course of laser-induced CNV and evaluated the effect of an intravitreal injection of vasohibin-1 protein or the genetic knockout (KO) of vasohibin-1 on laser-induced CNV in rodents.

METHODS

Animals

The procedures used in all the animal experiments adhered to the guidelines of the ARVO Statement for the Use of Animals in Ophthalmic and Vision Research and were approved by the Animal Care Committee of Tohoku University Graduate School of Medicine. Male mice between 8 to 12 weeks of age were used. Homozygous vasohibin-1 gene KO mice on a C57BL/6J background were generated by gene targeting, as described.[29] Wild-type (WT) C57BL/6J mice served as controls. For all procedures, the animals were anesthetized with an intraperitoneal injection of 30 mg/kg pentobarbital, and the pupils were dilated with topical 2.5% phenylephrine and 1% tropicamide.

One hundred sixty-two mice were used. Four untreated mice and 12 mice at 4, 14, and 28 days (four per group) after the laser application were used for immunohistochemistry. Thirty mice (five groups, six mice in each group) were used for reverse transcription-polymerase chain reaction (RT-PCR) to determine the natural course of the laser-induced CNV. Twenty-four mice (four groups: untreated, 4, 7, and 14 days after laser application; six mice in each group) for RT-PCR after vasohibin-1 or vehicle injection (24 mice) into the vitreous for laser-induced CNV (eight mice; WT and KO for RT-PCR of vasohibin-1; 4 mice each group); 24 mice (four groups: vasohibin-1 and vehicle injection for WT and KO mice, respectively; six mice in each group) for fluorescein angiography; and 36 mice (six groups with 0, 1, 10, and 100 ng vasohibin-1 injection for WT and vehicle and vasohibin-1 for KO; six mice in each group) for choroidal flat mounts.

Expression and Purification of Human Vasohibin-1 Protein

Human vasohibin-1 gene with optimized codons for *Escherichia coli* expression was cloned into pET-32 LIC/Xa (Novagen, Madison, WI). The resultant expression plasmid encoded vasohibin-1 with a sequence of GSNSPLAMAISDPNSSSVDKLAAALEHHHHHHH at its C terminus, as a thioredoxin fusion protein. *E. coli* BL21(DE3) transformants were cultivated at 37°C in TB medium (2.4% yeast extract, 1.2% tryptone, 1.25% K_2HPO_4, 0.23% KH_2PO_4, 500 mg/mL polypropylene glycol 2000, and 50 μg/mL ampicillin [pH 7.0]) supplemented with 4% glycerol, and the expression was induced by addition of 1 mM isopropyl-β-D-thiogalactopyranoside (OD_{650} = 5). After 16 hours of cultivation, the cells were harvested and disrupted in 20 mM sodium phosphate buffer (pH 7.6), containing 0.5 M NaCl and 1 mM phenylmethylsulfonyl fluoride (PMSF) in a high-pressure homogenizer. The inclusion bodies were collected, washed with the same buffer, and solubilized in 20 mM sodium phosphate buffer (pH 8.0), containing 0.5 M NaCl, 1 mM PMSF, 5 mM 2-mercaptoethanol, 60 mM imidazole, and 7 M guanidine HCl. The soluble fraction was loaded onto a Ni chelating Sepharose column (GE Health care, Princeton, NJ) which was equilibrated with the solubilization buffer. Vasohibin-1 fusion protein was eluted with 20 mM sodium phosphate buffer (pH 8.0), containing 0.5 M NaCl, 1 mM PMSF, 5 mM 2-mercaptoethanol, 300 mM imidazole, and 8 M urea. The eluted protein fraction was then dialyzed against 20 mM glycine-HCl buffer (pH 3.5) and digested with blood coagulation factor Xa (Novagen) for 1 hour at 25°C after the addition of the reaction buffer. The released vasohibin-1 was collected as the insoluble fraction, solubilized, and purified with Ni chelating Sepharose by a method used for fusion proteins. Vasohibin-1 was then collected as an insoluble fraction after dialysis against 20 mM Tris-HCl buffer (pH 8.0), resolubilized in 25 mM sodium phosphate (pH 7.2) containing 4 M urea, loaded onto a Q Sepharose column (GE Health care), and eluted by linearly increasing the NaCl concentration to 1 M. After vasohibin-1 was dialyzed against 20 mM glycine-HCl buffer (pH 3.5), the protein fraction was recovered as an insoluble fraction by addition of 1 M Tris-HCl buffer (pH 8.0) to 20% volume of the above solution. Vasohibin-1 was resolubilized with 50 mM Tris-HCl buffer containing 50 mM NaCl, 5 mM Tris(2-carboxyethyl)phosphine, 0.5 mM EDTA, 5% glycerol, and 4.4% *N*-lauroylsarcosine (pH 8.0) and was dialyzed twice against 20 mM sodium phosphate buffer (pH 8.0) and once with PBS, each for at least a day.

The protein concentration was determined by the Bradford method with a protein assay kit (Bio-Rad Laboratories, Hercules, CA), with bovine serum albumin as the standard protein.

Experimental CNV

An Argon green laser, with a slit lamp delivery system (Ultima 2000SE; Lumenis, Yokneam, Israel) and a coverslip as a contact lens, was used to rupture the choroidal membrane.[30–32] The laser settings were 50-μm diameter, 0.05-second duration, and 150-mW intensity. For fluorescein angiography and choroidal flat-mount examinations, three burns were made in the peripapillary region in a standardized fashion, and each burn was approximately one to two disc diameters from the optic disc.

For RT-PCR and immunohistochemistry, three burns were made around the optic disc with the burns separated by one to two disc diameters. Only eyes in which subretinal bubbles were formed indicating a rupture of the Bruch membrane were studied.

Immunohistochemistry

WT mice with laser-induced CNV lesions were studied on days 4, 14, and 28 after laser burn for immunostaining of vasohibin-1 (n = 4 eyes/group). All procedures were performed at room temperature unless otherwise stated. The eyes were enucleated and fixed for 12 hours in 4% paraformaldehyde (PFA) at 4°C and cryoprotected by successive incubations in 10%, 20%, and 30% sucrose dissolved in saline, for 12 hours each at 4°C. The tissues were immersed in OCT compound (Tissue-Tek; Sakura Finetek, Torrance, CA) and frozen in acetone in a dry ice bath. The frozen eyes were sectioned at 10 μm with a cryostat. Adjacent sections were stained with hematoxylin and eosin (HE).

For double staining with vasohibin-1, antibodies against CD-31 (marker for ECs), CD68 (marker for macrophage), α-smooth muscle actin (αSMA, maker for dedifferentiated RPE), and cytokeratin (marker for RPE) were used. Mouse eyes were enucleated, immersed in OCT compound and frozen in acetone in a dry ice bath. The frozen eyes were sectioned at 10 μm with a cryostat, dried, and fixed in methanol for 10 minutes. After blocking, mouse monoclonal antibodies against mouse vasohibin-1 (1:400)[29] and rat monoclonal antibodies against mouse CD-31 (a marker for ECs; 1:100; BD Biosciences, San Jose, CA), mouse monoclonal anti-CD68 antibody (a marker for macrophages; 1:400; Dako, Hamburg, Germany), mouse monoclonal anti-α-smooth muscle antibody (αSMA, maker for dedifferentiated RPE, 1:400; Thermo Fisher Scientific Inc., Waltham, MA), mouse monoclonal anti-mouse pan-cytokeratin (a marker for RPE; 1:200; pan-cytokeratins/cytokeratin 18 clone CY90; CK18, 1:10, Sigma-Aldrich, St. Louis, MO) were applied to the sections overnight at 4°C. For control experiments, preimmune mouse IgG was used instead of the primary antibody. The sections were incubated in Alexa Fluor 594-conjugated anti-mouse IgG (1:400; Invitrogen, Eugene, OR) and Alexa Fluor 488-conjugated anti-rat IgG (1:100; Invitrogen) for 30 minutes. The sections were washed three times with PBS between each step. The slides were counterstained with 4, 6-diamino-1phenylindole (DAPI; Vector Laboratories, Burlingame, CA) and were photographed with a fluorescence microscope (model FW4000, ver. 1.2.1; Leica Microsystems Japan, Tokyo, Japan).

Preparation of Total RNA and Real-Time Reverse Transcription-Polymerase Chain Reaction

For semiquantitative RT-PCR, the eyes of male WT mice were enucleated on days 4, 7, 14, and 28 after the laser burns (n = 6 eyes/group).

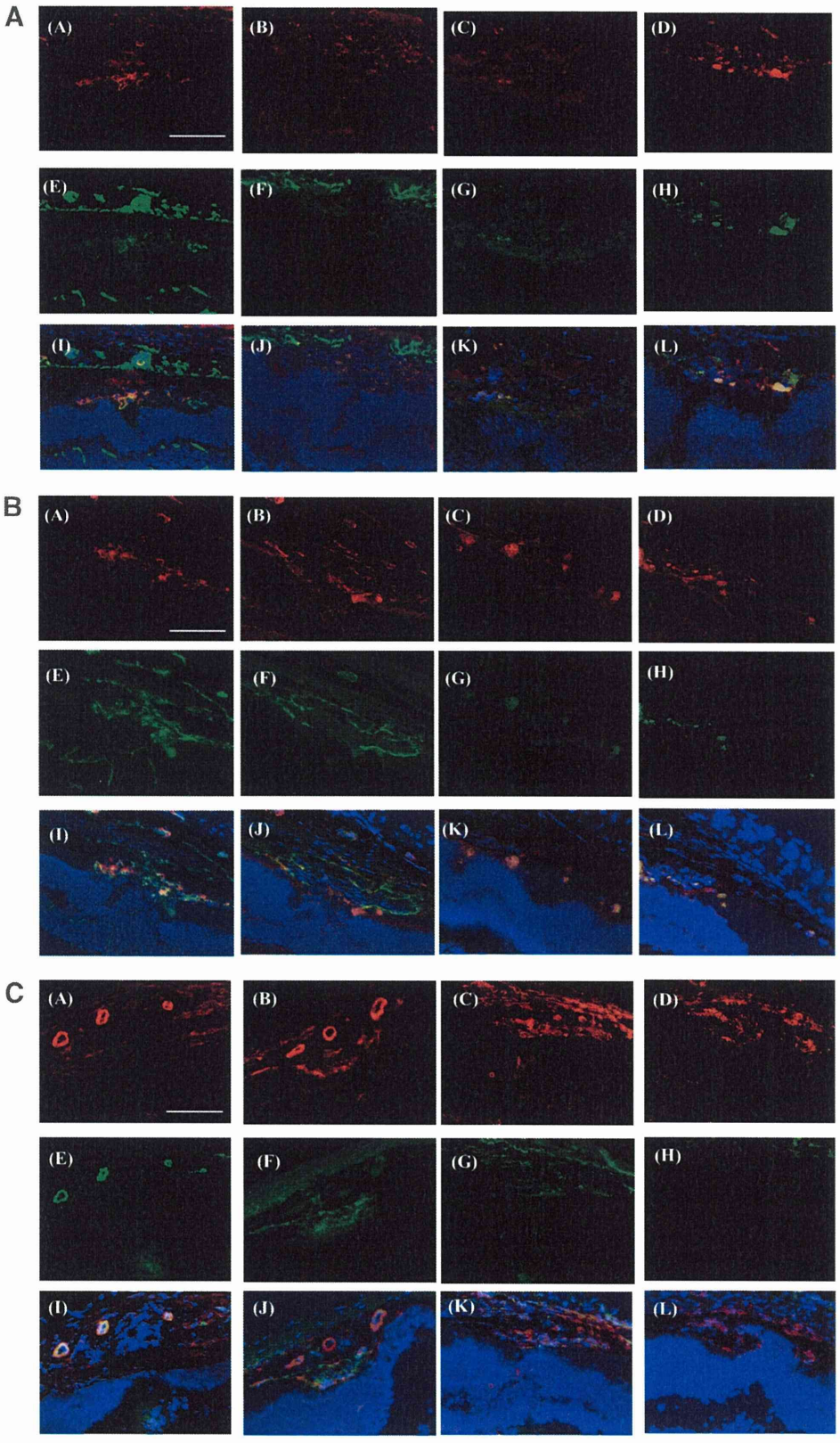

FIGURE 1. H&E staining and immunohistochemistry of laser-induced experimental CNV membranes. (**A**) H&E staining of a mouse eye at 4 days after laser application. A fusiform-shaped CNV is present. Immunohistochemistry for vasohibin-1 in mouse CNV lesions at 4 (**1.1**), 14 (**1.2**), and 28 (**1.3**) days after laser application is shown. (**A–D**) Vasohibin-1, (**E**) anti-CD68, (**F**) anti-cytokeratin, (**G**) anti-α smooth muscle actin (αSMA), and (**H**) anti-CD31, respectively. (**I–L**) Merged images. Vasohibin-1 was observed on these days, although it seems more intensive on day 28. On day 4, vasohibin was co-expressed with CD68-positive macrophages (**1.1A**, **1.1E**, **1.1I**) and CD31-positive endothelial cells (**1.1D**, **1.1H**, **1.1L**). These findings are also observed on day 14 after laser application (**1.2A**, **1.2E**, **1.2I**, **1.2D**, **1.2H**, **1.2L**). Further vasohibin-1 is co-expressed on αSMA-positive dedifferentiated RPE (**1.2C**, **1.2G**, **1.2K**) and partially with cytokeratin-positive RPE (**1.2B**, **1.2F**, **1.2J**). On day 28, vasohibin-1-positive cells were observed on CD31-positive choroidal endothelial cells (**1.3D**, **1.3H**, **1.3L**). CD68-positive macrophages were rarely seen on day 28 (**1.3A**, **1.3E**, **1.3I**). Cytokeratin-positive RPE was absent at the laser burned area on day 4 (**1.1F**), but gradually increased on day 14 (**1.2F**) and covered the CNV on day 28 (**1.3F**). None of these signals was observed with the control IgG. Bar, 20 μm.

Untreated eyes of WT and vasohibin-1 KO mice were also examined for the expression of vasohibin-1 (n = 4 eyes/group). The anterior segment, muscles, optic nerve, and entire retina were removed to isolate the eye cup which included the RPE-choroid-sclera complex. Each tissue was separately mixed with denaturing solution, and mRNA was prepared (QuickPrep micromRNA Purification Kit; Amersham Biosciences, Buckinghamshire, UK), according to the manufacturer's instructions. The purified mRNA was reverse-transcribed to cDNA using

(First-Strand cDNA Synthesis Kit; Amersham Biosciences). One microliter of cDNA was used for real-time PCR amplification on a thermocycler (Light Cycler; Roche, Meylan, France, and the Light Cycler FastStart DNA Master SYBR Green I Reagent Kit; Roche).

The sequences of the PCR primer pairs were: VEGF, 5′-TCT GCT CTC TTG GGT GCA AT-3′ (forward) and 5′-TTC CGG TGA GAG GTC CGG TT-3′ (reverse); vasohibin-1, 5′-GAT TCC CAT ACC AAG TGT GCC-3′ (forward), and 5′-ATG TGG CGG AAG TAG TTC CC-3′ (reverse); VEGFR1, 5′-GAGGAGGATGAGGGTGTCTATAGGT-3ACC AAG TGT GCC 5′-GTGATCAGCTCCAGGTTTGACTT-3-3ACC AAG TGT-VEGFR2, 5′-GCCCTGCCTGTGGTCTCACTAC-33-3ACC AAG TGT G5′-CAAAGCATTGCCCATTCGAT-3′ (reverse); PEDF, 5′-AGCTGAACATCGAA-CAGAGT-3′ (forward) and 5′-CGAAGTTTCCTCTCAAACAC-3′ (reverse); glyceraldehyde-3-phosphate-dehydrogenase (GAPDH), 5′-AAG GTG AAG GTC GGA GTC AA-3′ (forward), 5′-TTG AGG TCA ATG AAG GGG TC-3′.

The PCR conditions were: 95°C for 10 minutes; 95°C for 10 seconds; hybridization temperature for 10 seconds (VEGF, 66°C; vasohibin-1, 62°C; VEGFR1-1, 57°C; VEGFR2, 56°C; PEDF, 50°C; and GAPDH, 55°C); and 72°C for 10 seconds. The second step was repeated for 45 cycles. All data were normalized to GAPDH expression, thus giving the relative expression level.

Intravitreal Injection of Recombinant Vasohibin Protein

Male WT mice were injected intravitreally in both eyes with 1, 10, or 100 ng/1 μL recombinant vasohibin-1 protein[24–26,29] 4 days after the laser burn. One microliter of PBS was used as vehicle. The mice were anesthetized, the pupils were dilated, and the intravitreal injections were made with a 32-gauge needle attached to a 5-μL glass syringe (Hamilton, Reno, NV). The needle was passed through the sclera just behind the limbus into the vitreous cavity.

Fluorescein Angiography

Fluorescein angiography (FA) was used to determine the activity of the CNV lesion and to investigate the efficacy of vasohibin-1 protein injection in both WT and vasohibin-1 KO mice (n = 8 eyes/group).[30] FA was performed with a camera and imaging system (Genesis-Df; Kowa, Tokyo, Japan) 2 weeks after the laser photocoagulation. Photographs were taken with a 20-D lens in contact with the fundus camera lens after an intraperitoneal injection of 0.1 mL of 2% fluorescein sodium (Sigma-Aldrich). Two retinal specialists (RW, TA) evaluated the angiograms in a masked fashion. Lesions were graded according to an established scheme: 0, no leakage with faint hyperfluorescence or mottled fluorescence without leakage; 1, questionable leakage with hyperfluorescent lesion but no increase in size or intensity; 2A, leaky with hyperfluorescence increasing in intensity but not in size; and 2B, pathologically significant leakage with hyperfluorescence increasing in intensity and in size.[31] The CNV activity in the FA images was calculated for each of the three burns in each eye and summed.

Fluorescein-Labeled Dextran Perfusion and Choroidal Flat-Mount Preparation

The size of the CNV lesion was measured in choroidal flat mounts to compare vasohibin-1-deficient mice to WT mice and to investigate the efficacy of vasohibin-1 protein injection (n = 10 eyes/group). On day 14, after the laser application, the mice were perfused with 0.5 mL PBS containing 50 mg/mL fluorescein-labeled dextran (FITC-dextran; MW 2×10^6; Sigma Aldrich). The eyes were removed and fixed for 30 minutes in 4% phosphate-buffered PFA. The cornea and lens were removed, and the entire retina was carefully dissected from the eye cup. Radial cuts (four to six) were made from the edge to the equator, and the eye cup of the RPE-choroid-sclera complex was flat mounted (Permalfuor; Beckman Coulter, Fullerton, CA) with the sclera side facing down. Flat mounts were examined by fluorescence microscopy (model FW4000, ver. 1.2.1; Leica Microsystems Japan), and the total area of each CNV associated with each burn was measured. The CNV lesions were identified by the fluorescent blood vessels on the choroid-retinal interface circumscribed by a region lacking fluorescence.[31,32]

Statistical Analyses

Analysis of variance (ANOVA) with the Scheffé test for post hoc analysis was used to examine the differences in the relative expression levels of each gene. Differences in the incidence of grade 2B lesions between WT and KO mice, and between different dosages of intravitreal vasohibin-1 injections were analyzed by χ^2 tests. The size of CNV was compared between groups using the Student's two-sample t-tests.

Results

Histology and Immunostaining of CNV

We followed the natural course of laser-induced CNVs in the WT mice. The HE-stained sections of WT mice showed the same pattern in the development of CNV as described in another study.[32] On day 4 after the laser application, a fusiform-shaped lesion developed that consisted primarily of pigment-laden cells, fibroblasts, ECs, and RPE cells. Small new vessels containing red blood cells were present in parts of the lesion. On days 7 and 14, the lesion was larger and the blood vessels had increased in size and number (data not shown).

Vasohibin-1 was detected in CD31-positive cells on all days examined (Figs. 1.1, 1.2, 1.3: A, E, I). However, the expression seemed to be stronger on day 28 after the laser burn. Vasohibin-1 was also detected in CD68-positive cells on days 4 (Figs. 1.1A, 1.1E, 1.1I) and 14 (Figs. 1.2A, 1.2E, 1.2I). CD68-positive

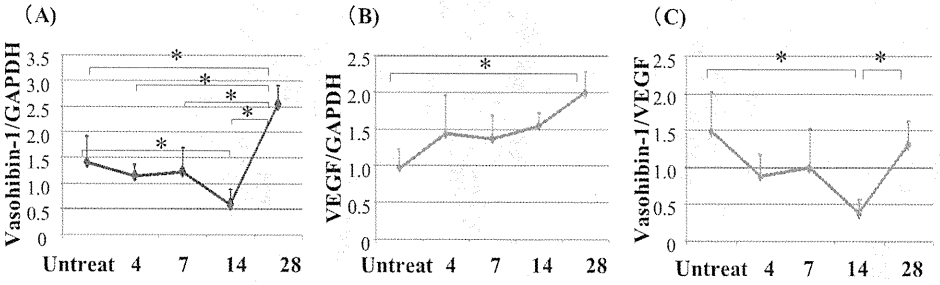

Figure 2. Semiquantitative RT-PCR of wild-type mouse eyes after laser application. The level of expression of vasohibin-1 (**A**) and vascular endothelial growth factor (VEGF) (**B**) is normalized to that of glyceraldehyde-3-phosphate-dehydrogenase (GAPDH). Vasohibin-1 expression decreases until 14 days after laser application, and then markedly increases on day 28. VEGF expression increases gradually until 28 day after laser application. The ratio of vasohibin-1/VEGF expression decreased until 14 days after laser and then increased at day 28 (**C**). $^*P < 0.05$.

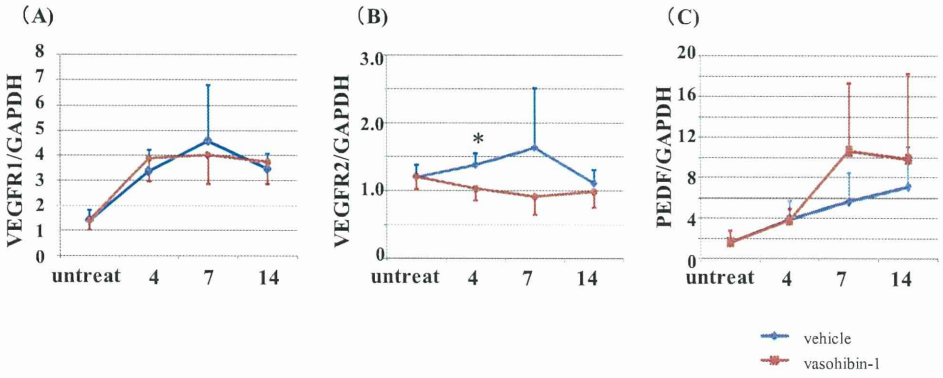

FIGURE 3. Semiquantitative RT-PCR for VEGFR1, VEGFR2, and PEDF are shown. VEGFR1 expression is not significantly different between vasohibin-1- and vehicle-treated eyes (**A**). Significantly lower levels of VEGFR2 expression were observed on day 4 after laser application between vasohibin-1- and vehicle-treated eyes (**B**, *asterisk*). PEDF expression was not significantly different between vasohibin-1- and vehicle-treated eyes (**C**).

cells were rarely observed on day 28. Vasohibin-1 was also detected in αSMA-positive cells on day 14 (Figs. 1.2C, 1.2G, 1.2K). A weak expression of vasohibin-1 was also detected in cytokeratin-positive cells on days 14 and 28 (Figs. 1.2, 1.3: B, F, J). Our preliminary study showed that RPE cell lines, such as RPE-J and ARPE, expressed the vasohibin-1 gene (data not shown). Our results therefore showed that ECs and macrophages, dedifferentiated RPE, and perhaps some of the differentiated RPE may express vasohibin-1.

Real-Time RT-PCR

The results of real-time RT-PCR in WT mice are shown in Figure 2. The level of vasohibin-1 expression decreased until day 14 after the laser application and then was markedly increased on day 28 (Fig. 2A). Thus, the mean ratio of the mRNA expression of vasohibin-1/GAPDH was 1.403 ± 0.503 before the laser application, 1.14 ± 0.239 on day 4 after laser application, 1.226 ± 0.080 on day 7, 0.593 ± 0.119 on day 14, and 2.552 ± 0.147 on day 28. Statistical analyses showed that vasohibin-1 expression on day 28 was significantly higher than in untreated eyes ($P = 0.001$) or on days 4 ($P < 0.0001$), 7 ($P = 0.0001$), and 14 ($P < 0.0001$). The lower expression observed on day 14 than that of untreated eyes was significant ($P = 0.0277$).

Conversely, the VEGF expression increased gradually until 28 days after the laser application (Fig. 2B). Thus, the mean ratio of the mRNA level of VEGF was 0.962 ± 0.265 before laser application, and 1.436 ± 0.522 at day 4, 1.358 ± 0.335 at day 7, 1.539 ± 0.175 at day 14, and 1.996 ± 0.289 at day 28. At day 28 after laser application, the VEGF levels were significantly higher than in the untreated eyes ($P = 0.0006$). The ratio of vasohibin/VEGF expression (Fig. 2C) was 1.484 ± 0.54 without laser, 0.877 ± 0.298 at day 4 after laser, 0.989 ± 0.537 at day 7, 0.384 ± 0.178, at day 14, and 1.314 ± 0.316 on day 28. Thus, the ratio decreased until day 14 after the laser application and then returned to the normal level on day 28. The vasohibin/VEGF level on day 14 was significantly lower than that in the untreated eyes ($P = 0.0022$) and on day 28 ($P = 0.0116$).

The results of real-time PCR for VEGFR1 in WT mice showed that VEGFR1 expression was not significantly different between vasohibin-1 injected and vehicle injected eyes (Fig. 3A). The expression of VEGFR2 in vasohibin-1-treated eyes was significantly lower than that in vehicle-treated eyes 4 days after the laser application (Fig. 3B, asterisk; $P = 0.013$). The expression of PEDF in the vasohibin-1 treated eyes was not significantly different from that in vehicle-treated eyes (Fig. 3C).

Angiographic Leakage from CNV

Fluorescein angiography showed that an intravitreal injection of 10 ng recombinant vasohibin-1 protein on day 4 after laser application led to a significant reduction in the size of the CNV. On day 14, significant pathologic leakage (grade 2B lesions) was observed in 57.1% of the lesions in control mice, but in only 8.3% of the lesions in the treated mice ($P = 0.0002$; Fig. 4).

We performed the same experiments in vasohibin-1 KO mice. The fundus, histologic, and ERG examinations showed that the morphologic architecture and function of vasohibin-1 KO mice did not differ from those of wild-type mice under normal conditions (data not shown). Vasohibin was expressed in retinal and choroidal vessels by immunostaining and RT-PCR analyses. Conversely, vasohibin-1 was not detected in the mutant eyes (Fig. 5A). Comparisons of the fluorescein angiograms showed that vasohibin-1 KO mice developed larger and leakier

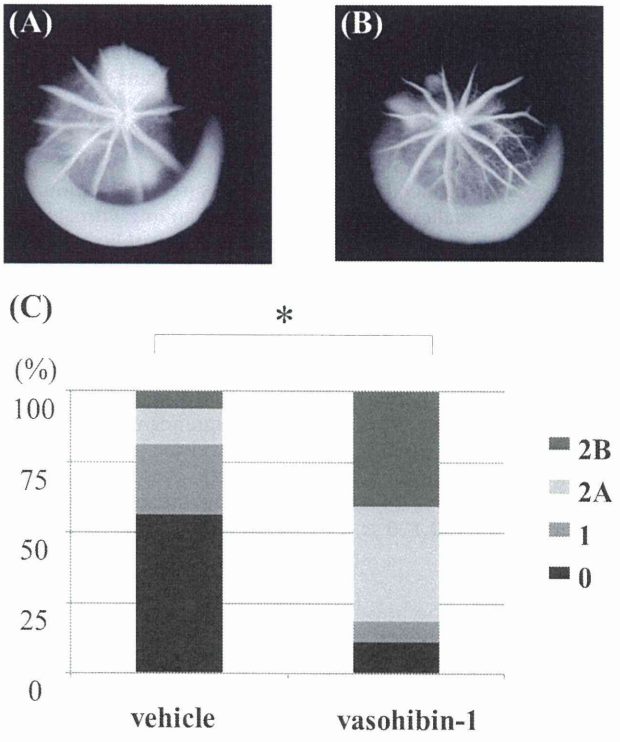

FIGURE 4. Angiographic leakage from CNV lesions with and without intravitreal injection of 10 ng recombinant vasohibin-1 protein 4 days after laser application. (**A**) Representative fluorescein angiogram of vehicle-injected eyes. Active CNV can be seen as a large hyperfluorescent area. (**B**) Representative fluorescein angiogram of vasohibin-1-injected eyes. Small and less leaky CNVs indicate the inhibitory effect of vasohibin-1. (**C**) Histogram of angiographic leakage grades. A significantly lower numbers of grade 2B lesions occur in vasohibin-1-injected eyes than in control eyes 2 weeks after laser induction ($P < 0.001$, χ^2 test).

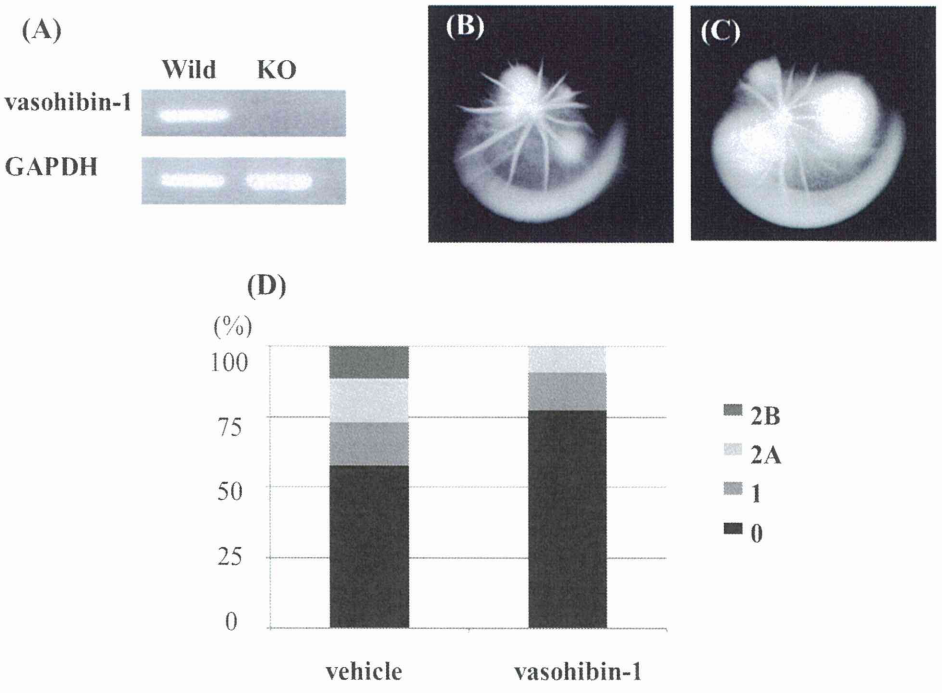

FIGURE 5. (**A**) RT-PCR analysis of vasohibin-1 and glyceraldehyde-3-phosphate-dehydrogenase (GAPDH) mRNA in the eyes of wild-type or KO mice. Vasohibin-1 was not detected in the KO eye. Angiographic leakage from CNV lesions in the eyes of wild-type or vasohibin-1 KO mice. (**B**, **C**) Representative fluorescein angiogram of wild-type eyes and vasohibin-1-KO eyes, respectively, showing larger and leakier CNV lesions in KO compared with wild-type. (**D**) Histogram of angiographic leakage grades. More grade 2B lesions occurred in vasohibin-1-KO eyes than in wild-type eyes 2 weeks after laser induction, but the difference is not statistically significant ($P = 0.097$, χ^2 test).

CNVs than did the WT mice (Figs. 5B, 5C). On day 14, grade 2B lesions were observed in 55.0% of the lesions in WT mice and a higher percentage (81.2%) of 2B lesions were detected in the vasohibin-1 deficient mice. However, the difference in the percentages of grade 2B lesions was not significant ($P = 0.097$, Fig. 5D).

Size of CNVs in Flat Mounts

The size of the induced CNV lesions measured in flat-mounted choroids was smaller in eyes that received an intravitreal injection of vasohibin-1 protein on day 4 after laser application than in the controls (Fig. 6). Thus, the size of the CNV in the controls was 49,926 ± 11,837 μm^2; 34,019 ± 10,048 μm^2 (68.1% of control) after 1 ng, 20,465 ± 6541 μm^2 (40.9% of control) after 10 ng, and 23,733 ± 5116 μm^2 (47.5% of control) after 100 ng of vasohibin-1. The differences between control and 1 ng, between control and 10 ng, and between control and 100 ng were all statistically significant ($P = 0.0002$, <0.0000001, and <0.0000001, respectively).

The mean size of the CNV lesions in the eyes of vasohibin-1 KO mice (105,140 ± 34,447 μm^2) was significantly larger than that in the WT (49,176 ± 15,455 μm^2; $P = 0.00001$; Fig. 7).

Discussion

Vasohibin-1 is expressed in a wide range of tissues and organs in embryos and adults.[24,33] It is also expressed on human CNV membranes,[28] proliferative membranes of diabetic retinopathy,[34] and blood vessels in tumors.[35] Our results showed that vasohibin-1 was expressed, not only on the endothelial cells but also on macrophages, dedifferentiated RPE cells, and probably on RPE cells. The expression seemed to increase after the laser application. When we examined the vasohibin-1 expression on day 28 after laser application, strong vasohibin-1 expression was observed only on the CNV lesion, although weak expression was always observed on the RPE cells. αSMA-positive dedifferentiated RPE cells also expressed vasohibin-1 on day 14, and histologic examination showed that regressed CNV lesions were covered with cytokeratin-positive RPE cells on day 28. These results show that vasohibin-1 expression may play a role in the regression of CNV, as we reported.[28]

When the CNV was created around the optic disc (three spots in each eyes), each spot did not have the same degree of FA leakage. From our experimental design, it was very difficult to detect significant differences in the vasohibin-1/VEGF ratio for each spot. Alternatively, we determined the vasohibin-1/VEGF ratio during the following days. RT-PCR showed that the vasohibin-1 expression was significantly decreased on 14 days after laser application and then increased above normal level on day 28. This result agrees with the reports that laser-induced CNV lesion enlarges and matures between days 7 to 14 after laser application.[31,36] The results of RT-PCR for vasohibin-1/VEGF ratio show comparable results. From these results, we suggest that the growth and the maturation of the CNV lesions may partially correlate with the vasohibin-1 and VEGF expression levels.

Although vasohibin-1 expression is stimulated by VEGF, VEGF receptor 2, and the protein kinase C delta (PKCδ) pathway,[27] other proangiogenic and antiangiogenic factors may modify the expression of vasohibin-1 during the course of the CNV development. It has been reported that not only VEGF, but also bFGF, placenta growth factor, and hepatocyte growth factor increase the expression of vasohibin-1.[24,27] TNF-α, interleukin (IL)-1, and hypoxia inhibit the VEGF-stimulated vasohibin-1 expression in vitro.[24,27] The macrophage-like mononuclear cells in human CNVs have been reported to produce TNF-α and IL-1β.[8] Shi et al.[37] reported the expression of TNF-α was 4.57-fold higher in the choroid and RPE of eyes with a laser-induced CNV than in the eyes of controls. In addition, pretreatment of these eyes with anti-TNF-α agents significantly reduced the size of the CNV and the pathologic fluorescein leakage. We also observed macrophages in the CNVs until day 14 which showed that the CNV lesions were still active but rarely on day 28 when the CNV had already regressed.

It has been reported that choroidal blood flow and the permeability of Bruch's membrane is decreased in the eyes of the elderly, especially patients with AMD, resulting in a hypoxic environment surrounding the choroidal ECs.[38–40] Hyp-

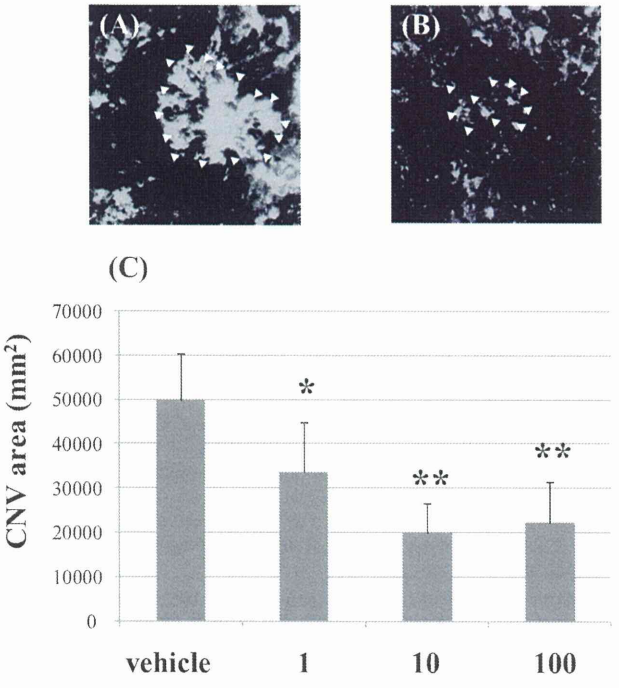

FIGURE 6. Size of CNV membranes, with or without intravitreal injection of recombinant vasohibin-1 protein, 4 days after laser application. (**A**) Representative choroidal flat-mount photograph of vehicle-injected eyes. (**B**) Representative choroidal flat-mount photograph of eyes injected with 10 ng of vasohibin-1 protein. *Small arrowheads*: CNV lesion. (**C**) Choroidal flat-mount examination 2 weeks after laser induction after 1, 10, and 100 ng of vasohibin-1 protein suppresses the growth of the CNVs. Vasohibin-1 suppressed CNV at 32% by 1 ng, 59% by 10 ng, and 52% by 100 ng, when compared to that of vehicle injection. $^{*}P < 0.001$, $^{**}P < 0.0000001$, Student's two-sample *t*-tests compared with vehicle-injected eyes.

oxia increases the expression of VEGF and matrix metalloproteinase in choroidal ECs, and this may facilitate the formation and recurrences of CNVs.[41] Hypoxia may also change the vasohibin-1 expression. We suggest that the regulation of vasohibin-1 expression may change the natural course of CNV in patients with AMD.[28]

Our results showed that an intravitreal injection of vasohibin-1 significantly reduced the size of the CNVs, and vasohibin-1 KO mice had larger CNVs than that of WT mice. Ida et al.[42] reported that despite a continuous high expression of VEGF and its receptors, subretinal neovascularizations stopped growing and reached a plateau in rho/VEGF transgenic mice. These results show that not only the withdrawal of angiogenic stimulation by VEGF, but also antiangiogenic factors, including vasohibin-1, play a role in CNV regression during its natural course.

Many other endogenous antiangiogenic factors, such as PEDF, a 50-kDa noninhibitory member of the serine protease inhibitor gene family, must be considered.[43,44] PEDF is expressed in RPE cells, CNV membranes, corneal cells, and ciliary epithelial cells.[9,44] The concentration of PEDF in the vitreous and aqueous decreases with increasing age and is very low in AMD patients.[45] It has been reported that the level of PEDF in CNV membranes increases after stimulation of the VEGF receptor 1.[46] This effect may be a negative feedback loop against the VEGF-induced neovascularization. Studies using gene transfer have demonstrated that PEDF suppresses the development of CNVs.[47,48] Our real-time PCR results confirmed these findings that the expression of PEDF also increased during the CNV enlargement until day 14. The level of PEDF expression was opposite that of vasohibin-1 expression. However, vasohibin-1 injection did not induce significant differences in the PEDF expression from that obtained with vehicle injection. Vasohibin-1 was suspected to suppress CNV, in addition to PEDF signaling. Apte et al.[49] reported that low doses of PEDF are inhibitory in experimental CNV, whereas high doses enhance the development of neovascularization. A maximum dose of intravitreal 100 ng vasohibin-1, which is 10 times the amount with the maximum effect, did not reverse the effect of PEDF under our experimental conditions. Vasohibin-1 may be safer than PEDF for antiangiogenesis in our experimental condition.

Although a complete understanding of the angiogenic inhibition by vasohibin-1 has not been attained, Shen et al.[26] reported that vasohibin-1 suppressed retinal neovascularization and suggested that a downregulation of the VEGF receptor 2 gene may play some role in mediating its activity. Zhou et al.[50] reported a significant reduction of corneal neovascularization by alkali-treated mice cornea. They showed a significant decrease of in VEGFR2 gene expression during the experimental period and suggested that there is an important correlation in the downregulation of VEGFR2 and vasohibin-1. When we examined the gene expression of VEGFR1 and -R2, significantly less VEGFR2 expression was observed in the vasohibin-1-treated eyes at day 4 after laser application, although the results may have been affected by the number of animals ($n = 6$). Although we could not examine the VEGF-mediated tyrosine phosphorylation of VEGFR2 from our small samples, we suggest that external vasohibin-1 plays some role in the antiangiogenesis by a downregulation of VEGFR2, together with the earlier findings. These observations also imply a synergistic effect of anti-VEGF agents and vasohibin-1 against CNV growth.

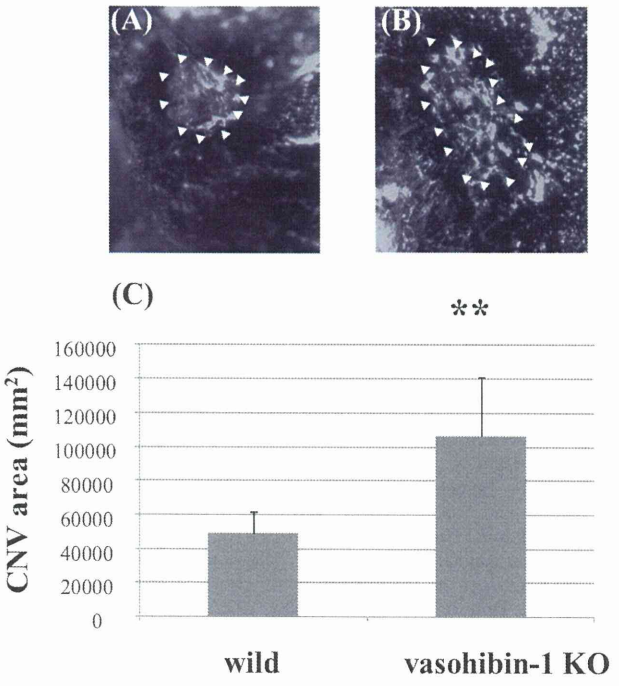

FIGURE 7. Size of CNV lesions in the eyes of wild-type or vasohibin-1-KO mice. (**A**) Representative choroidal flat-mount photograph of wild-type eye. (**B**) Representative choroidal flat-mount photograph of vasohibin-1-KO eye. *Arrowheads*: the CNV. (**C**) Choroidal flat-mount examination 2 weeks after laser induction shows CNVs in the eyes of vasohibin-1-KO mice are two times (213.8%) larger than that of wild-type eyes. $^{**}P < 0.0001$, Student's two-sample *t*-test, compared with wild-type eyes.

When we injected vasohibin-1 intravitreally on days 1, 4, and 7 after laser application, we found that eyes that received vasohibin-1 on day 4 had better results than those at the other days. This is the reason that we injected vasohibin-1 4 days after the laser application. Vasohibin is thought to work in an autocrine manner[24,25] with a small vasohibin-binding protein.[51] The half-life of vasohibin-1 is short, approximately 5 minutes (Sato Y, personal communication, 2010), after systemic application. However, the half-life of vasohibin-1 in the eye is unknown. It may be very short and may correlate with the timing of vasohibin-1 application at 4 days after laser application, under our experimental conditions. Alternatively, our experimental condition may have affected the results. In any case, when we consider the optimum day for the vasohibin injection, it may be different from that of anti-VEGF agents. This reason may be another explanation for the synergistic effect of anti-VEGF agents and vasohibin-1 against CNV growth.

In conclusion, the endogenous expression of vasohibin-1 is associated with the natural course of the development of a CNV. Vasohibin-1 was expressed on ECs, macrophages, and weakly on RPE cells, and especially on active CNV lesions. External vasohibin-1 application may alter the development of experimental mice CNVs, and we recommend that vasohibin-1 be considered to as a treatment to suppress CNV growth.

Acknowledgments

The authors thank Kota Sato and Haruka Seto for excellent technical assistance.

References

1. Klein R, Peto T, Bird AC, Vannewkirk MR. The epidemiology of age-related macular degeneration. *Am J Ophthalmol.* 2004;137:486–495.
2. Bressler NM, Bressler SB, Fine SL. Age-related macular degeneration. *Surv Ophthalmol.* 1998;32:375–413.
3. Amin R, Puklin JE, Frank RN. Growth factor localization in choroidal neovascular membranes of age-related macular degeneration. *Invest Ophthalmol Vis Sci.* 1994;35:3178–3188.
4. Frank RN, Amin RH, Eliott D, Puklin JE, Abrams GW. Basic fibroblast growth factor and vascular endothelial growth factor are present in epiretinal and choroidal neovascular membranes. *Am J Ophthalmol.* 1996;122:393–403.
5. Lopez PF, Sippy BD, Lambert M, Thach AB, Hinton DR. Transdifferentiated retinal pigment epithelial cells are immunoreactive for vascular endothelial growth factor in surgically excised age-related macular degeneration-related membranes. *Invest Ophthalmol Vis Sci.* 1996;37:855–868.
6. Kvanta A, Algvere PV, Berglin L, Seregard S. Subfoveal fibrovascular membranes in age-related macular degeneration express vascular endothelial growth factor. *Invest Ophthalmol Vis Sci.* 1996;37:1929–1934.
7. Otani A, Takagi H, Oh H, et al. Vascular endothelial growth factor family and receptor expression in human choroidal neovascular membranes. *Microvasc Res.* 2002;64:162–169.
8. Oh H, Takagi H, Takagi C, et al. The potential angiogenic role of macrophages in the formation of choroidal neovascular membranes. *Invest Ophthalmol Vis Sci.* 1999;40:1891–1898.
9. Matsuoka M, Ogata N, Otsuji T, et al. Expression of pigment epithelium derived factor and vascular endothelial growth factor in choroidal neovascular membranes and polypoidal choroidal vasculopathy. *Br J Ophthalmol.* 2004;88:809–815.
10. Grisanti S, Tatar O. The role of vascular endothelial growth factor and other endogenous interplayers in age-related macular degeneration. *Prog Retin Eye Res.* 2008;27:372–390.
11. Spilsbury K, Garrett KL, Shen WY, Constable IJ, Rakoczy PE. Overexpression of vascular endothelial growth factor (VEGF) in the retinal pigment epithelium leads to the development of choroidal neovascularization. *Am J Pathol.* 2000;157:135–144.
12. Krzystolik MG, Afshari MA, Adamis AP, et al. Prevention of experimental choroidal neovascularization with intravitreal anti-vascular endothelial growth factor antibody fragment. *Arch Ophthalmol.* 2002;120:338–346.
13. Rosenfeld PJ, Brown DM, Heier JS, et al. MARINA Study Group. Ranibizumab for neovascular age-related macular degeneration. *N Engl J Med.* 2006;355:1419–1431.
14. Regillo CD, Brown M, Abraham P, et al. PIER Study Group. Randomized, double-masked, sham-controlled trial of ranibizumab for neovascular age-related macular degeneration: PIER study year 1. *Am J Ophthalmol.* 2008;145:239–248.
15. Pilli S, Kotsolis A, Spaide RF, et al. Endophthalmitis associated with intravitreal anti-vascular endothelial growth factor therapy injections in an office setting. *Am J Ophthalmol.* 2008;145:879–882.
16. Lux A, Llacer H, Heussen FMA, Joussen AM. Non-responders to bevacizumab (Avastin) therapy of choroidal neovascular lesions. *Am J Ophthalmol.* 2007;91:1318–1322.
17. Alon T, Hemo I, Itin A, Pe'er J, Stone J, Keshet E. Vascular endothelial growth factor acts as a survival factor for newly formed retinal vessels and has implications for retinopathy of prematurity. *Nat Med.* 1995;1:1024–1028.
18. Robinson GS, Ju M, Shih SC, et al. Nonvascular role for VEGF: VEGFR1, 2 activity is critical for neural retinal development. *FASEB J.* 2001;15:1215–1217.
19. Marneros AG, Fan J, Yokoyama Y, Gerber HP, Ferrara N, Crouch RK, Olsen BR. Vascular endothelial growth factor expression in the retinal pigment epithelium is essential for choriocapillaris development and visual function. *Am J Pathol.* 2005;167:1451–1459.
20. Nishijima K, Ng YS, Zhong L, et al. Vascular endothelial growth factor-A is a survival factor for retinal neurons and a critical neuroprotectant during the adaptive response to ischemic injury. *Am J Pathol.* 2007;171:53–67.
21. Saint-Geniez M, Maharaj AS, Walshe TE, et al. Endogenous VEGF is required for visual function: evidence for a survival role on Müller cells and photoreceptors. *PLoS One.* 2008;3:e3554.
22. Boyer DS, Heier JS, Brown DM, et al. A phase IIIb study to evaluate the safety of ranibizumab in subjects with neovascular age-related macular degeneration. *Ophthalmology.* 2009;116:1731–1739.
23. Ueno S, Pease ME, Wersinger DM, et al. Prolonged blockade of VEGF family members does not cause identifiable damage to retinal neurons or vessels. *J Cell Physiol.* 2008;217:13–22.
24. Watanabe K, Hasegawa Y, Yamashita H, et al. Vasohibin as an endothelium-derived negative feedback regulator of angiogenesis. *J Clin Invest.* 2004;114:898–907.
25. Sonoda H, Ohta H, Watanabe K, et al. Multiple processing forms and their biological activities of a novel angiogenesis inhibitor vasohibin. *Biochem Biophys Res Commun.* 2006;342:640–646.
26. Shen J, Yang X, Xiao WH, et al. Vasohibin is up-regulated by VEGF in the retina and suppresses VEGF receptor 2 and retinal neovascularization. *FASEB J.* 2006;20:723–725.
27. Shimizu K, Watanabe K, Yamashita H, et al. Gene regulation of a novel angiogenesis inhibitor, vasohibin, in endothelial cells. *Biochem Biophys Res Commun.* 2005;327:700–706.
28. Wakusawa R, Abe T, Sato H, et al. Expression of vasohibin, an antiangiogenic factor, in human choroidal neovascular membranes. *Am J Ophthalmol.* 2008;146:235–243.
29. Kimura H, Miyashita H, Suzuki Y, et al. Distinctive localization and opposed roles of vasohibin-1 and vasohibin-2 in the regulation of angiogenesis. *Blood.* 2009;113:4810–4818.
30. Tobe T, Ortega S, Luna JD, et al. Targeted disruption of the FGF2 gene does not prevent choroidal neovascularization in a murine model. *Am J Pathol.* 1998;153:1641–1646.
31. Yu HG, Liu X, Kiss S, et al. Increased choroidal neovascularization following laser induction in mice lacking lysyl oxidase-like 1. *Invest Ophthalmol Vis Sci.* 2008;49:2599–2605.
32. Edelman JL, Castro MR. Quantitative image analysis of laser-induced choroidal neovascularization in rat. *Exp Eye Res.* 2000;71:523–533.
33. Nimmagadda S, Geetha-Loganathan P, Pröls F, et al. Expression pattern of vasohibin during chick development. *Dev Dyn.* 2007;236:1358–1362.

34. Sato H, Abe T, Wakusawa R, et al. Vitreous levels of vasohibin-1 and vascular endothelial growth factor in patients with proliferative diabetic retinopathy. *Diabetologia.* 2009;52:359–361.
35. Hosaka T, Kimura H, Heishi T, et al. Vasohibin-1 expression in endothelium of tumor blood vessels regulates angiogenesis. *Am J Pathol.* 2009;175:430–439.
36. Odergren A, Ming Y, Kvanta A. Photodynamic therapy of experimental choroidal neovascularization in the mouse. *Curr Eye Res.* 2006;31:765–774.
37. Shi X, Semkova I, Müther PS, et al. Inhibition of TNF-alpha reduces laser-induced choroidal neovascularization. *Exp Eye Res.* 2006;83:1325–1334.
38. Ito YN, Mori K, Young-Duvall J, Yoneya S. Aging changes of the choroidal dye filling pattern in indocyanine green angiography of normal subjects. *Retina.* 2001;21:237–242.
39. Ross RD, Barofsky JM, Cohen G, et al. Presumed macular choroidal watershed vascular filling, choroidal neovascularization, and systemic vascular disease in patients with age-related macular degeneration. *Am J Ophthalmol.* 1998;125:71–80.
40. Chen JC, Fitzke FW, Pauleikhoff D, Bird AC. Functional loss in age-related Bruch's membrane change with choroidal perfusion defect. *Invest Ophthalmol Vis Sci.* 1992;33:334–340.
41. Ottino P, Finley J, Rojo E, et al. Hypoxia activates matrix metalloproteinase expression and the VEGF system in monkey choroid-retinal endothelial cells: Involvement of cytosolic phospholipase A2 activity. 1: *Mol Vis.* 2004;10:341–350.
42. Ida H, Tobe T, Nambu H, et al. RPE cells modulate subretinal neovascularization, but do not cause regression in mice with sustained expression of VEGF. *Invest Ophthalmol Vis Sci.* 2003;44:5430–5437.
43. Dawson DW, Volpert OV, Gillis P, et al. Pigment epithelium-derived factor: a potent inhibitor of angiogenesis. *Science.* 1999;285:245–248.
44. Tong JP, Yao YF. Contribution of VEGF and PEDF to choroidal angiogenesis: a need for balanced expressions. *Clin Biochem.* 2006;39:267–276.
45. Holekamp NM, Bouck N, Volpert O. Pigment epithelium-derived factor is deficient in the vitreous of patients with choroidal neovascularization due to age-related macular degeneration. *Am J Ophthalmol.* 2002;134:220–227.
46. Ohno-Matsui K, Yoshida T, Uetama T, Mochizuki M, Morita I. Vascular endothelial growth factor upregulates pigment epithelium-derived factor expression via VEGFR-1 in human retinal pigment epithelial cells. *Biochem Biophys Res Commun.* 2003;303:962–967.
47. Mori K, Gehlbach P, Ando A, et al. Regression of ocular neovascularization in response to increased expression of pigment epithelium-derived factor. *Invest Ophthalmol Vis Sci.* 2002;43:2428–2434.
48. Campochiaro PA, Nguyen QD, Shah SM, et al. Adenoviral vector-delivered pigment epithelium-derived factor for neovascular age-related macular degeneration: results of a phase I clinical trial. *Hum Gene Ther.* 2006;17:167–176.
49. Apte RS, Barreiro RA, Duh E, Volpert O, Ferguson TA. Stimulation of neovascularization by the anti-angiogenic factor PEDF. *Invest Ophthalmol Vis Sci.* 2004;45:4491–4497.
50. Zhou SY, Xie ZL, Xiao O, et al. Inhibition of mouse alkali burn induced-corneal neovascularization by recombinant adenovirus encoding human vasohibin-1. *Mol Vis.* 2010;26:16:1389–1398.
51. Suzuki Y, Kobayashi M, Miyashita H, et al. Isolation of a small vasohibin-binding protein (SVBP) and its role in vasohibin secretion. *J Cell Sci.* 2010;123:3094–3101.

Biomaterials 32 (2011) 1950–1956

Contents lists available at ScienceDirect

Biomaterials

journal homepage: www.elsevier.com/locate/biomaterials

A scalable controlled-release device for transscleral drug delivery to the retina

Takeaki Kawashima [a,1], Nobuhiro Nagai [b,1], Hirokazu Kaji [a,c], Norihiro Kumasaka [b], Hideyuki Onami [d], Yumi Ishikawa [b], Noriko Osumi [e], Matsuhiko Nishizawa [a,c], Toshiaki Abe [b,*]

[a] Department of Bioengineering and Robotics, Graduate School of Engineering, Tohoku University, 6-6-01 Aramaki-Aoba, Aoba-ku, Sendai 980-8579, Japan
[b] Division of Clinical Cell Therapy, Center for Advanced Medical Research and Development, ART, Tohoku University Graduate School of Medicine, 2-1 Seiryo-machi, Aoba-ku, Sendai 980-8575, Japan
[c] JST, CREST, Sanbancho, Chiyoda-ku, Tokyo 102-0075, Japan
[d] Department of Ophthalmology, Tohoku University Graduate School of Medicine, 1-1 Seiryo-machi, Aoba-ku, Sendai 980-8574, Japan
[e] Division of Developmental Neuroscience, Center for Neuroscience, ART, Tohoku University Graduate School of Medicine, 2-1 Seiryo-machi, Aoba-ku, Sendai 980-8575, Japan

ARTICLE INFO

Article history:
Received 13 October 2010
Accepted 3 November 2010
Available online 26 November 2010

Keywords:
Drug-delivery system
Transscleral delivery
Controlled release
Retinal neuroprotection
Polyethylene glycol

ABSTRACT

A transscleral drug-delivery device, designed for the administration of protein-type drugs, that consists of a drug reservoir covered with a controlled-release membrane was manufactured and tested. The controlled-release membrane is made of photopolymerized polyethylene glycol dimethacrylate (PEGDM) that contains interconnected collagen microparticles (COLs), which are the routes for drug permeation. The results showed that the release of 40-kDa FITC-dextran (FD40) was dependent on the COL concentration, which indicated that FD40 travelled through the membrane-embedded COLs. Additionally, the sustained-release drug formulations, FD40-loaded COLs and FD40-loaded COLs pelletized with PEGDM, fine-tuned the release of FD40. Capsules filled with COLs that contained recombinant human brain-derived neurotrophic factor (rhBDNF) released bioactive rhBDNF in a manner dependent on the membrane COL concentration, as was found for FD40 release. When capsules were sutured onto sclerae of rabbit eyes, FD40 was found to spread to the retinal pigment epithelium. Implantation of the device was easy, and it did not damage the eye tissues. In conclusion, our capsule is easily modified to accommodate different release rates for protein-type drugs by altering the membrane COL composition and/or drug formulation and can be implanted and removed with minor surgery. The device thus has great potential as a conduit for continuous, controlled drug release.

1. Introduction

The design of drug-delivery systems targeting the retina is a most challenging ophthalmological task. The principal delivery route currently in use is topical eye drop administration, but it delivers only low drug levels to the retina, and systemic drug delivery, e.g., intravenous delivery of Cytovene, a ganciclovir-type antiviral agent for cytomegalovirus [1], can produce toxic side effects. Although intravitreal delivery allows for high concentrations of a drug to be delivered directly to the retina, the necessary surgical procedure often requires repeated injections that can cause cataracts, retinal detachment, infection, and/or vitreous hemorrhage [2]. Therefore, transscleral delivery has emerged as a more attractive method for treating retinal disorders because it can deliver a drug locally and is less invasive [3,4]. Because of its large surface area and high degree of hydration, the sclera is permeable to drugs of different sizes (up to ~70 kDa) [5]. Transscleral drug-delivery systems that range in size from microparticles to polymeric implants have been tested [6]. However, most of these systems are made of biodegradable polymers. Drug release profiles for biodegradable devices generally have a tri-phasic release profile, i.e., an initial burst, a diffusional release phase, and a final burst [7]. This complex profile occurs because the polymers erode with time and, by doing so, affect drug dissolution. Thus, a non-biodegradable device that contains a drug reservoir sealed with a semipermeable membrane allows for sustained release and reduces the sizes of the bursts [8].

Neuroprotection from retinal degenerative diseases by neurotrophic factor delivery to the retina remains a challenge for ophthalmology [9]. Intraocular administrations of brain-derived neurotrophic factor (BDNF) [10], ciliary neurotrophic factor [11], and basic fibroblast growth factor [12], have been shown to rescue degenerating photoreceptor cells in animals. Additionally, we have demonstrated that the implantation of genetically modified iris pigment epithelial cells that secrete BDNF to the subretinal space

* Corresponding author. Tel./fax: +81 (0) 22 717 8234.
E-mail address: toshi@oph.med.tohoku.ac.jp (T. Abe).
[1] Equal contribution to this work.

0142-9612/$ – see front matter © 2010 Elsevier Ltd. All rights reserved.
doi:10.1016/j.biomaterials.2010.11.006

protect photoreceptors against phototoxicity [13]. However, suitable devices that specifically deliver neurotrophic factors continuously to the retina and with minimal invasiveness have yet to be developed. Therefore, we aimed to develop a membrane-based capsule that is implantable on the sclera (Fig. 1A) and would prolong the controlled delivery of BDNF or other protein-type drugs to the retina with zero-order kinetics. The designed capsule consists of two parts, a molded triethylene glycol dimethacrylate (TEGDM) reservoir to contain the drug and a new type of controlled-release membrane sealed around the top of the reservoir (Fig. 1B). TEGDM is a biomedical material that has been clinically used as a dental filler for the restoration of teeth [14]. The controlled-release membrane was produced by photopolymerizing a mixture of polyethylene glycol dimethacrylate (PEGDM) and collagen microparticles (COLs) (PEGDM/COL membrane). PEGDM has been successfully used by us [15] and several other groups [16,17] both *in vitro* and *in vivo* as a bio-inert scaffold material that can be easily molded into different substrate shapes and then annealed by UV crosslinking. The COLs are hydrogels containing a chemically crosslinked 0.8% (w/v) collagen network [18], which is permeable to molecules with molecular weights of <200 kDa. Drugs diffuse through the interconnected COLs embedded in the membrane. Additionally, the capsule can contain various formulations and dosages of a drug so that it can be used for many different biomedical applications. Herein, we report the fabrication, characterization, and implantation on rabbit sclerae of this transscleral drug-delivery device and demonstrate its applicability for the administration of protein-type drugs to the retina.

2. Materials and methods

2.1. Fabrication of the PEGDM/COL membrane

Mixtures (900 μl) of PEGDM prepolymer (M_n 750, Aldrich), 1% 2-hydroxy-2-methylpropiophenone, and COLs at concentrations of 0, 100, 300, or 500 mg/ml were poured individually into acrylic molds (3 × 3 × 0.1 cm) and photopolymerized with UV light that had an intensity of 11.5 mJ/cm^2 for 90 s (Lightningcure LCS, Hamamtsu Photonics) to produce membranes with thicknesses of 100 μm. COLs (average diameter, 8.7 μm) were prepared as described [18]. Briefly, 10 ml of a 1% (w/v) collagen solution (Nippon Meat Packers) was emulsified in 50 ml of liquid paraffin containing 0.3% (v/v) surfactant and stirred (600 rpm) at room temperature for 5 min. To crosslink the collagen, 1 ml of 50% (v/v) water-soluble carbodiimide (Dojindo) in water was added to the emulsified mixture and stirred (600 rpm) for 1 h. Then, 50 ml of 50% (v/v) ethanol was added into the mixture and mixed for 5 min to separate the COLs from the oil phase. The mixture was centrifuged at 3000 × g for 5 min, and the supernatant was discarded. Ethanol (50% v/v) was mixed with the COL pellet, and then the suspension was centrifuged (3000 × g for 5 min). After removing the supernatant, phosphate-buffered saline (PBS) was mixed with the COL pellet and then the suspension was centrifuged (3000 × g for 5 min). This procedure was repeated 3 times to remove residual ethanol.

2.2. Preparation of drug formulations

Three formulations that contained the drug mimic, 40-kDa fluorescein isothiocyanate dextran (FD40) plus PBS (F_{sol}), in COLs (F_{col}), or in COLs pelletized with PEGDM (F_{pel}) were prepared. For the preparation of F_{sol}, FD40 (Sigma) was dissolved in PBS at a concentration of 10 mg/ml. For the preparation of F_{col}, PBS solutions of

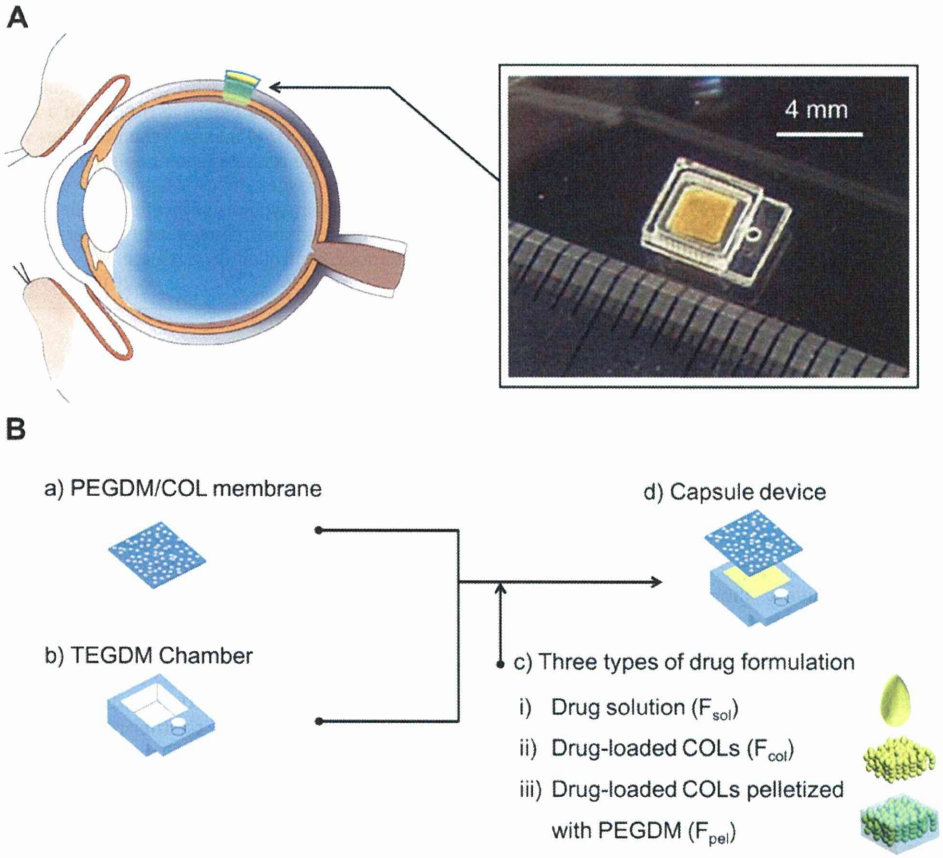

Fig. 1. (A) A transscleral drug-delivery device, designed for the administration of protein-type drugs. The photograph shows a capsule that contained FD40-loaded COLs pelletized with PEGDM and has a hole for suturing the capsule onto the sclera. (B) The capsule consists of a drug reservoir made of TEGDM and a controlled-release membrane made of photopolymerized PEGDM that contains COLs (PEGDM/COL membrane), which are the route for drug permeation. The capsule was designed so that various drug formulations could be contained in the reservoir.

COLs, which were obtained by centrifugation at 3000 × *g* for 30 min, were stirred in an equal volume of PBS that contained FD40 (20 mg/ml) for 24 h, and then the COLs were washed and centrifuged (3000 × *g* for 5 min) three times with PBS. For the preparation of F_{pel}, the FD40-loaded COLs in PBS (20 mg/ml FD40) were mixed with an equal volume of the PEGDM prepolymer and UV cured for 3 min. All drug formulations had the same amount of FD40 (10 mg/ml).

2.3. Fabrication of the capsule

A schematic of the capsule fabrication is shown in Fig. 1B. A polydimethylsiloxane master mold for the reservoir was first fabricated via a microfabrication technique that used an AutoCAD design and a micro-processing machine (Micro MC-2, PMT Co.). TEGDM prepolymer (M_w, 286.3; Aldrich) was UV cured in the mold for 3 min and peeled off to obtain a TEGDM reservoir. After loading a drug, the membrane was sealed to the reservoir by UV curing TEGDM prepolymer, which in polymerized form served as the adhesive, for 3 min.

2.4. SEM analysis

Samples were fixed with 2.5% glutaraldehyde and dehydrated first with ethanol and, subsequently, with isoamyl acetate. The samples were then dried fully in a critical point dryer (HCP-2; Hitachi Koki), coated with *Pt* using an ion coater (L350S-C; Anelva), and subjected to SEM. The SEM apparatus (VE-9800; Kyence) was operated at 5–20 kV.

2.5. In vitro release study

Modified Transwells were prepared by replacing their original porous membranes with PEGDM/COL membranes of various compositions (Fig. S2). Each drug formulation (100 μl) was placed in a Transwell and the complete systems were incubated in 400 μl of PBS at 37 °C. To estimate the amounts of FD40 that had diffused out of the Transwells, the fluorescent intensities of the PBS solutions were measured spectrofluorometrically (Fluoroscan Ascent; Thermo). For the release study that used recombinant human BDNF (rhBDNF), the capsules (reservoir interior, 5 × 5 × 2.2 mm; capsule exterior, 10 × 10 × 2.4 mm) were each filled with 40 μl of rhBDNF-loaded COLs in PBS and sealed with a membrane with a COL concentration of 0, 100, 300, or 500 mg/ml, and incubated in 1 ml of PBS at 37 °C. The amount of released rhBDNF was measured using the reagents of a BDNF-ELISA kit (Invitrogen) according to the manufacturer's instructions. Each test result is reported as the mean ± SD of three samples.

2.6. Western blotting

Immortalized retinal ganglion cells (RGC5 cells; a generous gift from Dr. N. Agarwal, University of North Texas Health Science Center, Fort Worth, TX) were maintained in Dulbecco's modified Eagle's medium (DMEM) (1 g glucose/l, Gibco) containing 10% fetal bovine serum (FBS; Gibco), L-glutamine (4 mM, Gibco), and a penicillin (100 U/ml)/streptomycin (100 mg/ml) solution (Sigma). RGC5 cells were plated into culture dishes (diameter; 60 mm, TPP) at a density of 1×10^4 cells/cm^2 and incubated in DMEM for 24 h. After starving the cells in DMEM that did not contain FBS (DMEM-f) for 12 h, the cells were exposed to conditioned DMEM-f that contained rhBDNF that had been released from a capsule into the medium (see below) or that had been spiked with rhBDNF (0, 0.1, 1, and 10 ng/ml) for 1 h. Cells were then scraped from the culture support and lysed with the reagents of a ProteoJET Cell Lysis kit (CosmoBio). Protein concentrations were determined using BCA protein assay kit reagents (Pierce). Electrophoresis was performed using 4–15% Tris-glycine gels (Biorad). Proteins were transferred to PVDF membranes using a semidry transferring system (Biorad). The membranes were blocked with 5% ECL blocking agent (GE Healthcare) and then incubated with a primary antibody against phosphorylated MAPK (1:1000; Cell Signaling) and subsequently with the secondary antibody, horseradish peroxidase-linked IgG (1:5000; Cell Signaling). After stripping the membranes of the antibodies for 10 min using the reagents of a Western Re-Probe kit (Jacksun Biotech), the membrane was probed, in a similar manner, for total MAPK (anti-MAPK antibodies, 1:1000; Cell Signaling). Bands were visualized using an enhanced chemiluminescence system (ECL Plus, GE Healthcare). Conditioned media were prepared as follows. Capsules that contained rhBDNF-loaded COLs were incubating in DMEM-f at 37 °C. The medium was replaced with fresh DMEM-f at day 3 and at week 1, 2, 3, and 4.

2.7. Implantation study

We used the eyes of six rabbits, each of which weighed between 1.8 and 2.5 kg. All animals were handled in accordance with the ARVO Statement for the Use of Animals in Ophthalmic and Vision Research after receiving approval from the Institutional Animal Care and Use Committee of the Tohoku University Environmental & Safety Committee (No.22MdA-220). The rabbits were anesthetized with ketamine hydrochloride (35 mg/kg) and xylazine hydrochloride (5 mg/kg). Their ocular surfaces were anesthetized with a topical instillation of 0.4% oxybuprocaine hydrochloride. A paralimbal conjunctival incision was made 5–8 mm from the temporal limbus. The capsules, which were loaded with F_{pel}, were sutured onto the left eyes at the sclerae with 10-0 nylon. The right eyes served as controls. At the third day of implantation, fluorescent images were captured using a handheld retinal camera for fluorescein angiography (Genesis-D, Kowa) to document the fluorescence distributions around the capsules and the sclerae. After implantation for 1 month, capsules from three rabbits were carefully removed and subjected to SEM. For histological examination, the other three rabbits were killed with an overdose of pentobarbital sodium 3 days after implantation, and their eyes were enucleated and frozen immediately in liquid nitrogen. After mounting the cryostat sections in a medium that contained 4,6-diamidino-2-phenylindole (Vectashield, Vector Lab), the distribution of FD40 was observed by fluorescent microscopy (DMI6000B, Leica).

2.8. Statistical analysis

Experimental data are presented as means ± SDs. The results were evaluated by the Student *t*-test. Differences were considered significant if $P < 0.05$.

3. Results and discussion

3.1. Device fabrication

The capsule consists of a separately fabricated PEGDM/COL membrane and a TEGDM reservoir (Fig. 1B). The membrane was prepared by UV curing a mixture of PEGDM and COLs. PEGDM is almost impermeable to macromolecules with molecular weights >40 kDa (see below); therefore, the COLs provide the route for drug permeation. Scanning electron microscopy (SEM) images were acquired to visualize the surfaces of membranes with different COL concentrations. The COLs are the round particles seen in Fig. 2A–C, and the surface density of these particles is proportional to the concentration of COLs in the corresponding unpolymerized PEGDM/COL mixture (Fig. S1). Additionally, cross-sectional SEM images showed the presence of interconnecting COLs when the COL concentration was >300 mg/ml (Fig. 2D–F). The interconnecting COLs increased in density with the concentration of the COLs. Therefore, we assumed that the drug-release rate could be controlled by changing the COL density in the membrane. Because, conventionally, semipermeable membranes are made by forming pores within the membrane i.e., solvent casting/salt leaching [19], phase separation [20], emulsion freeze-drying [21], and bubble formation [22], our method is different and therefore pioneering. For this type of membrane, there is no need to remove remaining porogens (COLs) after polymerization because the COLs act as the route for drug release.

The TEGDM reservoir was microfabricated using a polydimethylsiloxane master mold. Because photopolymerized TEGDM is impermeable to macromolecules (see below), the reservoir is a barrier that forces unidirectional drug release. After loading the drug, the membrane was placed over the reservoir and TEGDM prepolymer was UV cured along the reservoir/membrane intersection to provide a seal. Cross-sectional SEM images indicated that a tight seal was formed (Fig. 2G). The drug mimic, FD40 in PBS, did not leak from a capsule that consisted of a standard TEGDM reservoir and a PEGDM membrane that lacked COLs; therefore, the capsule had been completely sealed. The capsule was designed to contain various drug formulations and dosages. In this study, sustained-release drug formulations were encapsulated to prolong drug release by limiting the rate of drug dissolution within the reservoir (see below).

3.2. Release controllability

To demonstrate that drug release could be controlled by both the membrane and the drug formulation, modified Transwell inserts were each fitted with a membrane of defined COL concentration (Fig. S2) and loaded with one of three formulations: FD40 in PBS (F_{sol}, Fig. 3A), FD40 in COLs (F_{col}, Fig. 3B), or FD40 in COLs

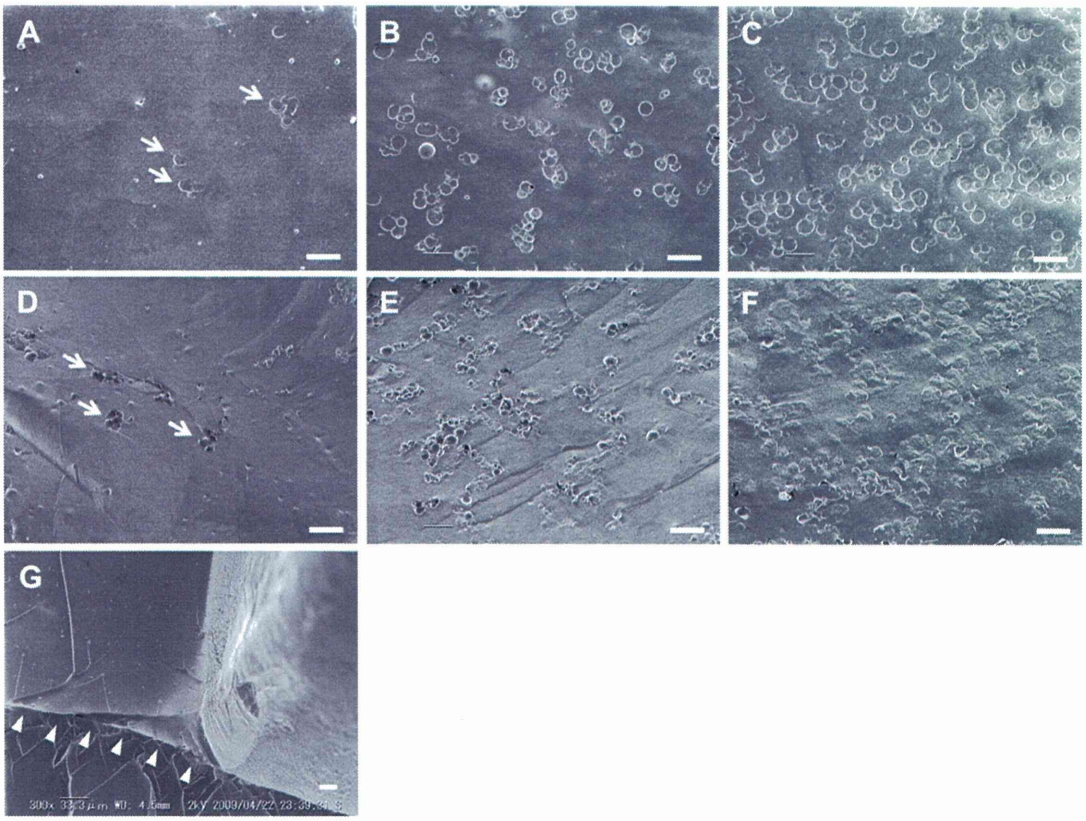

Fig. 2. Representative SEM images of (A–C) the surface and (D–F) cross sections of PEGDM/COL membranes that had COL concentrations of (A, D) 100 mg/ml, (B, E) 300 mg/ml, and (C, F) 500 mg/ml. The COLs are the round particles that form interconnecting structures throughout the membrane. Arrows point to COLs embedded in the membranes. (G) A cross-sectional SEM image of the capsule seal site that shows the formation of a tight seal. Arrowheads point to the seal site between the membrane and the capsule exterior. Bars: 20 μm.

pelletized with PEGDM (COL/PEGDM pellet) (F_{pel}, Fig. 3C). The COLs and the COL/PEGDM pellets, designed to be sustained-release drug formulations, were suspended in PBS. After placing the Transwells in PBS, FD40 release was monitored by assessing the increase in fluorescence in the external PBS solution with time. The results showed that the release of FD40 was always dependent on the COL concentration (Fig. 3A–C), which indicated that FD40 travelled through the membrane-embedded COLs. At the COL concentration of 100 mg/ml, the release kinetics was almost the same as the control (0 mg COL/ml). As shown by SEM analysis, almost no interconnected COLs existed in the 100 mg COL/ml membrane. When the membranes had been prepared with a COL concentration of 300 mg/ml, drug release followed zero-order kinetics. Additionally, F_{col} and F_{pel} behaved as sustained-release drug

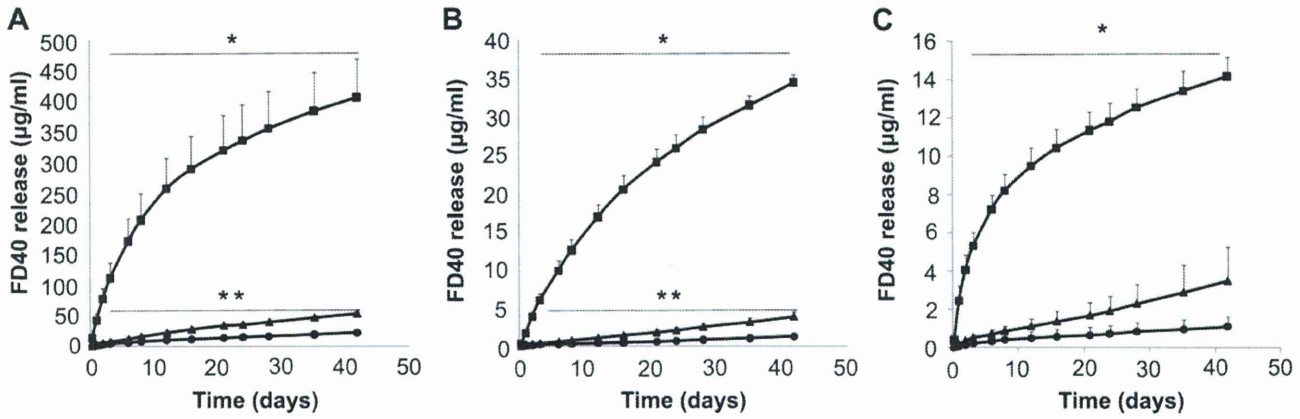

Fig. 3. Release of FD40 *in vitro*. The permeability of FD40 through PEGDM/COL membranes was studied using modified Transwells for which the PEGDM/COL membranes replaced the original Transwell membranes. The dependence of the release kinetics on the initial COL concentration for (A) FD40 in PBS (F_{sol}), (B) FD40-loaded COLs in PBS (F_{col}), and (C) FD40-loaded COLs pelletized with PEGDM in PBS (F_{pel}). The concentrations of the COLs were 100 mg/ml (circles), 300 mg/ml (triangles), and 500 mg/ml (squares). The release rate for FD40 through a membrane that did not contain COLs was almost the same as one that contained COLs at a concentration of 100 mg/ml. Error bars represent the standard deviations of three samples (error bars that are not visible are smaller than the symbols). The Means ± SDs are shown. $^{*}P < 0.05$ for 300 mg/ml vs. 500 mg/ml $^{**}P < 0.05$ for 100 mg/ml vs. 300 mg/ml.

formulations as they fine-tuned the release of FD40 in comparison with that of F_{sol}, perhaps because the COL and COL/PEGDM pellets, which cannot permeate the membrane, caused the reservoir solutions to have lower FD40 concentrations, which, in turn, decreased the steepness of the FD40 gradient from the reservoir to the exterior PBS solution. Therefore, the F_{col} and F_{pel} formulations, as sustained drug-release systems, improved the ability to control FD40 release by limiting the rate of FD40 dissolution, with the membrane controlling the diffusion rate via the COL tunnels. Consequently, the release of a drug can be controlled by the COL concentration in the membrane and the drug formulation.

3.3. Release mechanism

To further characterize the FD40 diffusion mechanism, we determined the diffusion coefficients for FD40 through 0.8% (w/v) crosslinked collagen (D_c), PEGDM (D_p), TEGDM (D_t), and water (D_w). D_c, D_p, and D_t were calculated using the FD40 diffusion rates through the gels (Fig. S3), and D_w was calculated using the Stokes–Einstein equation [23]. Because D_c (45.2 $\mu m^2/s$) was 1000 times larger than D_p (0.045 $\mu m^2/s$) and was smaller than D_w (67.9 $\mu m^2/s$), it appears that FD40 diffused through interconnected COLs in the membranes. If the COLs in the membrane are not interconnected, dead-ends are probably present that would inhibit the rate of drug release to the outside. However, once the COL density increases above a permeation threshold (>100 mg COL/ml), which was estimated by SEM as noted above (Fig. 2D–F), the COLs should be sufficiently interconnected that the number of dead-ends is reduced, and permeability is thereby increased. Because D_t was zero, FD40 cannot diffuse through the TEGDM reservoir, which enables unidirectional drug release.

3.4. In vitro BDNF release and bioactivity

To evaluate the release of the neurotrophic factor rhBDNF, capsules were filled with COLs that contained the protein and were tightly sealed with a membrane with a COL concentration of 0, 100, 300, or 500 mg/ml Fig. 4A presents the zero-order kinetic profiles found for rhBDNF release during a 6-week assay period. Apparently, the release kinetics of rhBDNF can be fine-tuned by varying the concentration of the COLs in a membrane in much the same manner as was found for FD40. Additionally, media that had been preincubated with capsules that contained rhBDNF induced the phosphorylation of mitogen-activated protein kinase (MAPK) in RGC5 cells when incubated with those cells as shown by western blotting of the cell extracts (Fig. 4B). BDNF is known to upregulate the expression of phosphorylated MAPK in retinal tissue [24]. In the present study, rhBDNF was found to phosphorylate MAPK in RGC5 cells in a dose-dependent manner by incubating the cells with media spiked with rhBDNF (Fig. 4C), which demonstrated that, when released from the capsule, rhBDNF retained its full activity.

Among the known neurotrophic factors, BDNF is the most potent survival factor for damaged retinal ganglion cells [10,25,26]. However, BDNF is currently administrated to the retina by intravitreal or subretinal injections in PBS [26], adenovirus vectors containing the BDNF gene [26,27], or genetically modified cells that secret BDNF [13,28]. Direct injections, however, result in extreme patient discomfort and complications arise caused by repeated injections or surgical procedures [2]. Because our capsule can contain various drug formulations, the encapsulation of the adenovirus vectors and the genetically modified cells might be possible and, as such, would represent a less invasive path than is currently available.

3.5. Implantation study

Our next challenge was to evaluate the capsule's ability to deliver a protein-type drug to the retina via the sclera. Capsules that had a reservoir (2.6 × 2.6 × 0.6 mm) filled with F_{pel} were sutured to the sclerae of three rabbits' left eyes with 10-0 nylon (Fig. 5A). The capsules abutted the sclerae but did not penetrate the conjunctivae or adjacent areas. Fig. 5B shows a fluorescent image of FD40 within a capsule, and Fig. 5C shows the release of FD40 locally at the sclera but not at the conjunctiva. This unidirectional release should reduce drug elimination by conjunctival lymphatic/blood clearance, thereby resulting in more effective delivery to the retina [29]. One month after implantation, the capsules remained sutured and neither the PEGDM of the membranes (Fig. 5D) nor the reservoirs had eroded (Fig. S4). The COLs in the membranes also survived with little biodegradation (Fig. 5D), most likely because the collagen molecules were stabilized by chemical crosslinking [18]. Although the capsules were loosely covered with connective tissue by the end of the trial, they were easily removed from the implant site. Routine ophthalmological examinations showed no eye-related toxic effects. Intense FD40 fluorescence in the sclerae adjacent to the implantation sites was observed (Fig. 5E). Furthermore, FD40 had migrated to the retinal pigment epithelium (RPE) and adjacent regions (Fig. 5F), which indicated that transscleral delivery of FD40 to the retina had been achieved. To the best of our knowledge, this is the first report that a macromolecule can be delivered to the

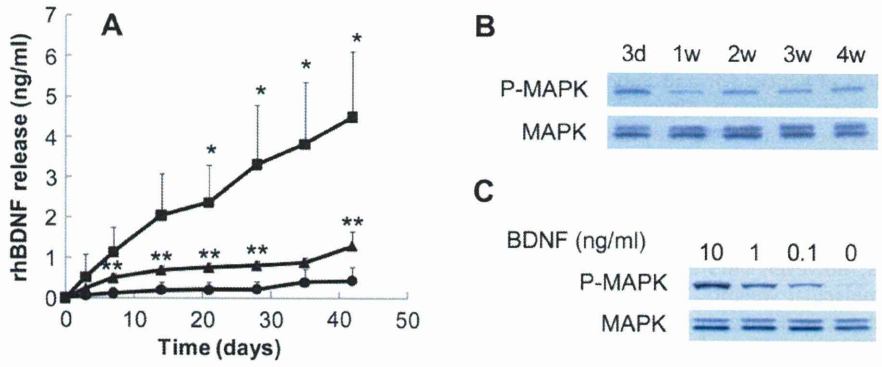

Fig. 4. Release of rhBDNF *in vitro*. (A) rhBDNF-loaded COLs in PBS were added to capsule reservoirs that sealed with a membrane with a COL concentration of 100 mg/ml (circles), 300 mg/ml (triangles), or 500 mg/ml (squares), and the release of rhBDNF was monitored using the reagents of a BDNF-ELISA kit. The release rate of rhBDNF through a PEGDM/COL membrane that contained 100 mg COL/ml was almost the same as one that contained no COLs. Means ± SDs are shown. $^*P < 0.05$ for 300 mg/ml vs. 500 mg/ml $^{**}P < 0.05$ for 100 mg/ml vs. 300 mg/ml. (B) Western blots of RGC5 cells extracts probed with antibody against phosphorylated MAPK (P-MAPK) and total MAPK. (C) The control study showed that rhBDNF could induce MAPK phosphorylation in RGC5 cells in a dose-dependent manner by incubating the cells with media spiked with rhBDNF.

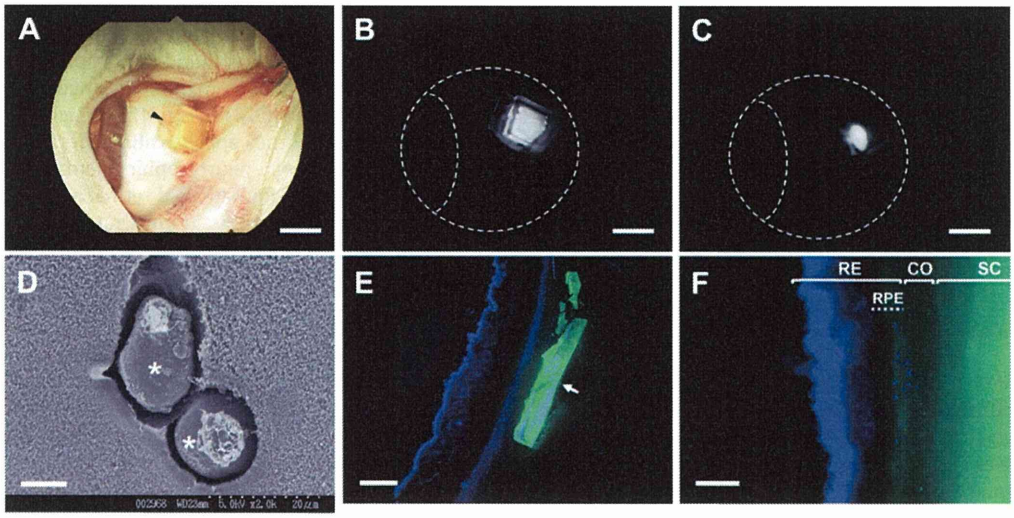

Fig. 5. Episcleral implantation of a capsule. (A) Image of a capsule sutured to the sclera of a rabbit eye 3 days after implantation. An arrowhead indicates the suture site. Fluorescent images around the sclera (B) immediately before and (C) after removal of the capsule 3 days after implantation. Fluorescence is visible as the white areas. (D) SEM image of a COL (asterisks) in the membrane of a used capsule that was removed 1 month after implantation. The COLs were not biodegraded. (E, F) The distribution of FD40 (green) in the retina and sclera around the implantation site 3 days after implantation (arrow: capsule). Cell nuclei were stained with 4,6-diamidino-2-phenylindole (blue). FD40 reached the retinal pigment epithelium. Abbreviations: sclera (SC), retinal pigment epithelium (RPE), choroid (CO), and retina (RE). Bars: 4 mm (A, B, and C), 10 μm (D), 400 μm (E), and 100 μm (F).

retina via a reservoir-based transscleral drug-delivery system, although quantification of the drug distribution still needs to be done. Proteins, as large as 50–75 kDa, penetrate into the choroid/RPE upon periocular injection [30]. Therefore, it may be possible to also deliver BDNF by the transscleral route. Given that the distribution of FD40 was somewhat concentrated at the RPE and adjacent regions, our device may be effective especially for lesions that surround the RPE. The capsule could also be used to deliver anti-angiogenic drugs, e.g., Lucentis and Macugen (for the treatment of age-related macular diseases) [31], to a lesion, e.g., the choroidal neovascular membrane, because delivery by this route will be less invasive and safer than are conventional intravitreal injections. Our non-biodegradable capsule should therefore be suitable for the transscleral delivery of protein-type drugs that require chronic suppressive-maintenance therapy over several weeks or months.

In summary, our capsule design incorporates features, outlined below, that have been absent from intraocular drug-delivery implant systems previously developed. First, the drug release kinetics can be controlled by changing the drug formulation and/or the membrane COL density so that the initial and final bursts are suppressed, which extends the release period. Second, the capsule is a scleral implantable device. To date, two ocular drug-delivery systems, Vitrasert [32] and Retisert [33], which are intravitreal sustained-release implants of ganciclovir and fluocinolone acetonide, respectively, have been marketed. Although these devices release the drugs at relatively constant rates, they must be surgically implanted in and later removed from the vitreous, which may cause complications or patient discomfort. Our capsule can be implanted and removed almost noninvasively by minor surgery. Third, most transscleral drug-delivery systems are designed to deliver low molecular weight drugs; however, ours appears able to deliver drugs of much greater molecular weights, i.e., protein-type drugs. Recent clinical trials and research have shown that many proteins are effective as drugs [9]. However, none of the available devices can deliver protein-type drugs in a controlled-release manner to the retina. Our capsule can be easily modified to accommodate different release rates for protein-type drugs by altering the membrane COL composition and/or drug formulation. Although this report demonstrated the release of only FD40 and BDNF, it should be possible to load and release low molecular weight drugs, protein-type drugs, and even drugs produced by encapsulated cells. The capsule thus has great potential for use in biomedical applications. Our future work will focus on preclinical animal studies to further assess the safety and effectiveness of the capsule.

4. Conclusion

This study reports the design and testing of a transscleral drug-delivery system that is implantable in the episclera and allows for controlled release of BDNF or other protein-type drugs with zero-order kinetics. Our microfabricated capsule consists of a drug reservoir sealed with a controlled-release membrane that contains interconnected COLs, which are the routes for drug permeation. The drug release kinetics can be controlled by changing the drug formulation and/or the membrane COL density so that the size of the bursts is reduced, which extends the release period. The capsule is designed to contain various drug formulations and dosages, allowing for a wide range of biomedical applications. The device thus has great potential as a conduit for continuous, controlled drug release.

Acknowledgments

This study was supported by the Takeda Science Foundation, the Research for Promoting Technological Seeds from the Japan Science and Technology Agency, and the Tohoku University Exploratory Research Program for Young Scientists, and was partially supported by Grants-in-Aid for Scientific Research B (20310070) and for Scientific Research on Priority Areas (21023002, 17659542, 18659508) from the Ministry of Education, Science, and Culture, Japan. Supporting information is available online or from the corresponding author.

Appendix

Figure with essential color discrimination. Fig. 4 of this article have parts that are difficult to interpret in black and white. The full

color image can be found in the online version, at doi:10.1016/j.biomaterials.2010.11.006.

Appendix. Supplementary data

Supplementary data related to this article can be found online at doi:10.1016/j.biomaterials.2010.11.006.

References

[1] Hughes PM, Olejnik O, Chang-Lin JE, Wilson CG. Topical and systemic drug delivery to the posterior segments. Adv Drug Deliv Rev 2005;57:2010–32.
[2] Geroski DH, Edelhauser HF. Transscleral drug delivery for posterior segment disease. Adv Drug Deliv Rev 2001;52:37–48.
[3] Ranta VP, Urtti A. Transscleral drug delivery to the posterior eye: prospects of pharmacokinetic modeling. Adv Drug Deliv Rev 2006;58:1164–81.
[4] Ambati J, Adamis AP. Transscleral drug delivery to the retina and choroid. Prog Retin Eye Res 2002;21:145–51.
[5] Olsen TW, Edelhauser HF, Lim JI, Geroski DH. Human scleral permeability. Effects of age, cryotherapy, transscleral diode laser, and surgical thinning. Invest Ophthalmol Vis Sci 1995;36:1893–903.
[6] Myles ME, Neumann DM, Hill JM. Recent progress in ocular drug delivery for posterior segment disease: emphasis on transscleral iontophoresis. Adv Drug Deliv Rev 2005;57:2063–79.
[7] Kunou N, Ogura Y, Yasukawa T, Kimura H, Miyamoto H, Honda Y, et al. Long-term sustained release of ganciclovir from biodegradable scleral implant for the treatment of cytomegalovirus retinitis. J Control Release 2000;68:263–71.
[8] McHugh AJ. The role of polymer membrane formation in sustained release drug delivery systems. J Control Release 2005;109:211–21.
[9] LaVail MM, Unoki K, Yasumura D, Matthes MT, Yancopoulos GD, Steinberg RH. Multiple growth factors, cytokines, and neurotrophins rescue photoreceptors from the damaging effects of constant light. Proc Natl Acad Sci U S A 1992; 89:11249–53.
[10] Di Polo A, Aigner LJ, Dunn RJ, Bray GM, Aguayo AJ. Prolonged delivery of brain-derived neurotrophic factor by adenovirus-infected Muller cells temporarily rescues injured retinal ganglion cells. Proc Natl Acad Sci U S A 1998;95:3978–83.
[11] Adamus G, Sugden B, Shiraga S, Timmers AM, Hauswirth WW. Anti-apoptotic effects of CNTF gene transfer on photoreceptor degeneration in experimental antibody-induced retinopathy. J Autoimmun 2003;21:121–9.
[12] Faktorovich EG, Steinberg RH, Yasumura D, Matthes MT, LaVail MM. Photoreceptor degeneration in inherited retinal dystrophy delayed by basic fibroblast growth factor. Nature 1990;347:83–6.
[13] Abe T, Yoshida M, Yoshioka Y, Wakusawa R, Tokita-Ishikawa Y, Seto H, et al. Iris pigment epithelial cell transplantation for degenerative retinal diseases. Prog Retin Eye Res 2007;26:302–21.
[14] Kalachandra S. Influence of fillers on the water sorption of composites. Dent Mater 1989;5:283–8.
[15] Hashimoto M, Kaji H, Nishizawa M. Selective capture of a specific cell type from mixed leucocytes in an electrode-integrated microfluidic device. Biosens Bioelectron 2009;24:2892–7.
[16] Lin-Gibson S, Bencherif S, Cooper JA, Wetzel SJ, Antonucci JM, Vogel BM, et al. Synthesis and characterization of PEG dimethacrylates and their hydrogels. Biomacromolecules 2004;5:1280–7.
[17] Weber LM, He J, Bradley B, Haskins K, Anseth KS. PEG-based hydrogels as an in vitro encapsulation platform for testing controlled beta-cell microenvironments. Acta Biomater 2006;2:1–8.
[18] Nagai N, Kumasaka N, Kawashima T, Kaji H, Nishizawa M, Abe T. Preparation and characterization of collagen microspheres for sustained release of VEGF. J Mater Sci Mater Med 2010;21:1891–8.
[19] Meier MM, Kanis LA, Soldi V. Characterization and drug-permeation profiles of microporous and dense cellulose acetate membranes: influence of plasticizer and pore forming agent. Int J Pharm 2004;278:99–110.
[20] Vogelaar L, Lammertink RG, Barsema JN, Nijdam W, Bolhuis-Versteeg LA, van Rijn CJ, et al. Phase separation micromolding: a new generic approach for microstructuring various materials. Small 2005;1:645–55.
[21] Grinberg O, Binderman I, Bahar H, Zilberman M. Highly porous bioresorbable scaffolds with controlled release of bioactive agents for tissue-regeneration applications. Acta Biomater 2010;6:1278–87.
[22] Yoon JJ, Park TG. Degradation behaviors of biodegradable macroporous scaffolds prepared by gas foaming of effervescent salts. J Biomed Mater Res 2001;55:401–8.
[23] Brandl F, Kastner F, Gschwind RM, Blunk T, Tessmar J, Gopferich A. Hydrogel-based drug delivery systems: comparison of drug diffusivity and release kinetics. J Control Release 2010;142:221–8.
[24] Klocker N, Kermer P, Weishaupt JH, Labes M, Ankerhold R, Bahr M. Brain-derived neurotrophic factor-mediated neuroprotection of adult rat retinal ganglion cells in vivo does not exclusively depend on phosphatidyl-inositol-3'-kinase/protein kinase B signaling. J Neurosci 2000;20:6962–7.
[25] Pernet V, Di Polo A. Synergistic action of brain-derived neurotrophic factor and lens injury promotes retinal ganglion cell survival, but leads to optic nerve dystrophy in vivo. Brain 2006;129:1014–26.
[26] Mansour-Robaey S, Clarke DB, Wang YC, Bray GM, Aguayo AJ. Effects of ocular injury and administration of brain-derived neurotrophic factor on survival and regrowth of axotomized retinal ganglion cells. Proc Natl Acad Sci U S A 1994;91:1632–6.
[27] Martin KR, Quigley HA, Zack DJ, Levkovitch-Verbin H, Kielczewski J, Valenta D, et al. Gene therapy with brain-derived neurotrophic factor as a protection: retinal ganglion cells in a rat glaucoma model. Invest Ophthalmol Vis Sci 2003;44:4357–65.
[28] Harper MM, Adamson L, Blits B, Bunge MB, Grozdanic SD, Sakaguchi DS. Brain-derived neurotrophic factor released from engineered mesenchymal stem cells attenuates glutamate- and hydrogen peroxide-mediated death of staurosporine-differentiated RGC-5 cells. Exp Eye Res 2009;89:538–48.
[29] Robinson MR, Lee SS, Kim H, Kim S, Lutz RJ, Galban C, et al. A rabbit model for assessing the ocular barriers to the transscleral delivery of triamcinolone acetonide. Exp Eye Res 2006;82:479–87.
[30] Demetriades AM, Deering T, Liu H, Lu L, Gehlbach P, Packer JD, et al. Transscleral delivery of antiangiogenic proteins. J Ocul Pharmacol Ther 2008;24: 70–9.
[31] Wong TY, Liew G, Mitchell P. Clinical update: new treatments for age-related macular degeneration. Lancet 2007;370:204–6.
[32] Sanborn GE, Anand R, Torti RE, Nightingale SD, Cal SX, Yates B, et al. Sustained-release ganciclovir therapy for treatment of cytomegalovirus retinitis. Use of an intravitreal device. Arch Ophthalmol 1992;110:188–95.
[33] Jaffe GJ, Martin D, Callanan D, Pearson PA, Levy B, Comstock T. Fluocinolone acetonide implant (Retisert) for noninfectious posterior uveitis: thirty-four-week results of a multicenter randomized clinical study. Ophthalmology 2006;113:1020–7.